INTERNATIONAL ENERGY AGENCY

IEA
SOLAR R&D

solar heating and
cooling programme

Characterization of Evacuated Collectors, Arrays, and Collection Subsystems

A Report of Task VI:
The Performance of Solar Heating, Cooling, and Hot Water Systems Using Evacuated Collectors

June 1986

Characterization of Evacuated Collectors, Arrays, and Collection Subsystems

A Report of Task VI: The Performance of Solar Heating, Cooling, and Hot Water Systems Using Evacuated Collectors

Professor Olivier Guisan
University of Geneva
Switzerland

Dr. Andre Mermoud
University of Geneva
Switzerland

Dr. Bernard Lachal
University of Geneva
Switzerland

Dr. Olivier Rudaz
University of Geneva
Switzerland

ACKNOWLEDGEMENTS

This report was written as part of research activity contracted by the Swiss Federal Energy Office. Financial help was also provided by the National Energy Research Foundation in Switzerland. We wish to acknowledge the contributions of information from other Task VI installations. Those contributing were

- United States
  Bill Duff and
  Karen Den Braven
- Sweden
  Bengt Perers and
  Heimo Zinko
- the Netherlands
  Chris Van Koppen and
  Bart Veltkamp
- Federal Republic of Germany
  Klaus Vanoli and
  Konrad Schreitmüller
- Commission of European Communities
  Dolf Van Hattem
- Canada
  Bill Carscallen,
  M. Chandrashekar and
  Hubert Taube
- Australia
  Dick Collins,
  Enn Mannik and
  Roland Schmid.

TABLE OF CONTENTS

1. INTRODUCTION

Task VI of the International Energy Agency Solar Heating and Cooling Program is a multinational research project that deals with the performance of evacuated collectors in systems. The study of twelve highly instrumented solar installations ranging from single family residential heating and cooling to large industrial applications makes up the Task. All the major evacuated collector types have been used. In six years of research, many analytical approaches and much specific technical information have evolved from the need to understand, explain, and compare experimental results. The Task assembled much of this material into this report characterizing evacuated collector modules, arrays, and collection subsystems. Not only should the reader be able to see the value of this material in analyzing the performance of solar energy systems, but also in formulating models and design tools.

Analyses have focused on the collector module, array, and collection subsystem because these are the common elements of solar energy systems and their performance and characteristics can be more or less directly compared without the complicating ambiguities of different size storages, possibilities of energy losses, and differing manners and patterns of energy end use.

Good arguments can be made that a single tube should be considered the collector and, in fact, single large evacuated tubes which are the performance equivalent of three square meter flat plate collectors have been produced. However, the Task has chosen the manifolded array of evacuated tubes as supplied by the collector manufacturer as the single collector module. Performance specifications for a single module generally come from the manufacturer or independent ponctual tests, not from Task measurements. The collector array boundaries are established by the array inlet and outlet temperature sensors. The array is made up of one or more single collector modules, intercollector module piping, and any additional array manifolding. The collection subsystem can be made up of one or more collector arrays, interarray piping, and piping to either storage, the rest of the system, or direct use. The boundaries of the collection subsystem are established by inlet and outlet temperature sensors.

Through the next three chapters this report progresses from the single collector module to the collection subsystem. The characterizations are mainly for instantaneous and steady state performance. Studying and characterizing collectors, arrays, and collection subsystems in detail as given in these chapters leads to the possibility of a generalized daily characterization which can be used as the basis for simple accurate system performance modeling. This possibility is discussed in the final chapter of this report.

2. SINGLE ETC MODULE CHARACTERISTICS

Tables 2-1 through 2-5 at the end of this section display the technical information on the collectors used in Task VI experiments. The following subsections will explain common precise definitions used in this report.

2.1 COLLECTOR AREA DEFINITION AND OTHER CONVENTIONS

IEA Task VI adopted the collector aperture area as a unique and unambiguous reference for all quantities normalized to the collector area. These quantities include collector efficiency and energy flows.

Task VI defines the collector aperture area as

$$A = L \cdot W \ ^{*} \qquad [m^2]$$

where L = exposed transparent part along collector tubes, excluding boxes, headers and so forth.
W = width of the collector module = n · p
n = number of tubes
p = distance between the centers of adjacent tubes, or pitch.
θ = tilt angle of the absorber plane with respect to the collector plane.

Most participants deal with untilted absorbers, but two recent Swiss experiments involve tilted absorbers. This report will show later that absorber tilt angle effects can be accounted for within the "incidence angle modifier" factor.

When normalized to an area, all Task VI figures refer to the aperture area. Any quantity normalized to the aperture area can be normalized to gross area, absorber area, or any other area by multiplying by the ratio "aperture area" to "other area." For instance, for the collector efficiency

$$\eta(\text{absorber area}) = \eta(\text{aperture area}) \cdot \frac{\text{aperture area}}{\text{absorber area}}$$

Other important Task VI conventions are that the absorber area corresponds to one side of the absorber when flat and to the entire area when cylindrical, and that the array aperture area is simply the sum of collector aperture areas.

---

* From the beginning of the Task through 1984, the aperture area definition included a cos θ factor, where θ is the tilt angle of the planar absorber surface. The Task included θ in the definition to account for Japanese installation where θ was relatively small. Subsequently, it was felt that the figures produced could be subject to misinterpretations. For example, if θ equals 90 degrees in the former definition, A equals zero. This means that such a collector would have infinite efficiency.

2.2 COLLECTOR TEMPERATURES

From the beginning, the Task adopted average collector fluid temperature as the relevant collector temperature for analysis and reporting. That is,

$$T_f \cong \frac{1}{2} (T_{in} + T_{out}) \qquad [K]$$

where T_{in} and T_{out} are the fluid temperatures at the collector inlet and outlet.

By doing so, we eliminated any confusion created by the "heat removal factor" F_R that is involved when adopting T_{in} instead of T_f. The obvious advantage in doing this is that collector efficiency no longer changes with the fluid flow rate. Collector efficiencies depend only on physical characteristics and ambient conditions and may then be directly compared.

In accordance with common practice, we use the collector efficiency factor F' to translate collector absorber temperature to average collector fluid temperature.

The inlet temperature may be useful in a few cases. We will see later that this temperature does not apply when looking at collector efficiencies in detail.

The average collector fluid temperature applies as long as T_{in} and T_{out} do not differ greatly, which is the case in most Task VI experiments.

2.3 COLLECTOR THERMAL CAPACITANCE

It is important to consider collector thermal capacitance as it can be a significant factor in the daily performance of some collector types and some systems, especially large arrays. Capacitance can hide some of the energy collected from the collection subsystem and, as the magnitude of the hidden energy can vary depending on such factors as load, it must be accounted for.

Collector thermal capacitance can be evaluated from the capacitances of its components, including the external glass tube. Collector thermal capacitance is calculated as

$$(M \cdot C)_{ETC} = \sum_i m_i \cdot c_i + \frac{U_c}{U_\infty} (m \cdot c)_{glass} \qquad [J/K]$$

where m_i = mass of the absorber, fluid, piping, and other components [kg]
and
c_i = specific heat of the absorber, fluid, piping, and other components. [J/kg·K]

A ratio of heat loss coefficients modifies the glass thermal capacity contribution as shown below

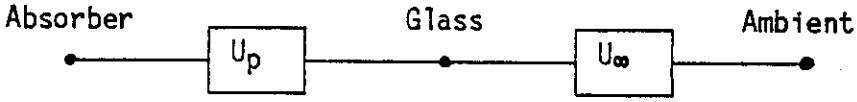

$$U_C = 1 \,/\, (1/U_p + 1/U_\infty) \qquad [W/K]$$

where U_p, U_∞, U_C refer to the same object, that is 1 tube or 1 collector.

In the case of ETC's, U_p is dominated by radiative exchanges and U_∞ is related to convection and radiation between the glass tube and the environment. For instance, for Corning CORTEC collectors, where the glass thickness is 2.7 mm, the glass contribution amounts to about 15 percent of the total collector capacitance, including fluid inventory.

We deal with insulation around the manifold and piping in the same way. This is also the case for arrays, subsystems, and other components of the system.

2.4 USUAL EXPRESSIONS OF COLLECTOR EFFICIENCY

Collector efficiency is usually written as

$$\eta_C = \frac{\dot{Q}}{I} = F' \left(\overline{\tau\alpha} - \frac{U_L \cdot \Delta T}{I}\right), \qquad \Delta T = T_f - T_a \qquad (1)$$

where F' = collector efficiency factor
$\dot{Q}$ = heat power from collector [W/m²]
$\overline{\tau\alpha}$ = optical efficiency
U_L = heat loss factor [W/m²K]
T_f = fluid temperature $\simeq (T_{in} + T_{out})/2$ [K]
T_a = ambient temperature and [K]
I = solar radiation on collector plane. [W/m²]

As stated previously, the reference area is the aperture area. Quantities normalized to the reference area are $\dot{Q}$, I, $\overline{\tau\alpha}$ and U_L.

When U_L is assumed to be a constant, expression (1) can be represented graphically in two equivalent ways as shown in Figure 1. Under this assumption the efficiency curve is a unique line and the power curves are a set of parallel lines equally spaced for equal ΔT variations. Various properties may be deduced from this Figure. For example, the point A is a stagnation point $\Delta T = I \cdot \overline{\tau\alpha}/U_L$ for a given value of I, or a radiation threshold $I = \Delta T \cdot U_L/\overline{\tau\alpha}$ for a given value of ΔT. Other properties are shown in the figure.

The collector efficiency factor F' involves the heat transfer from absorber to fluid. The factor incorporates the fin efficiency and the heat transfer from the fin base to the fluid. Let us consider the following cases:

Figure 1. Two Equivalent Representations of Collector Efficiency

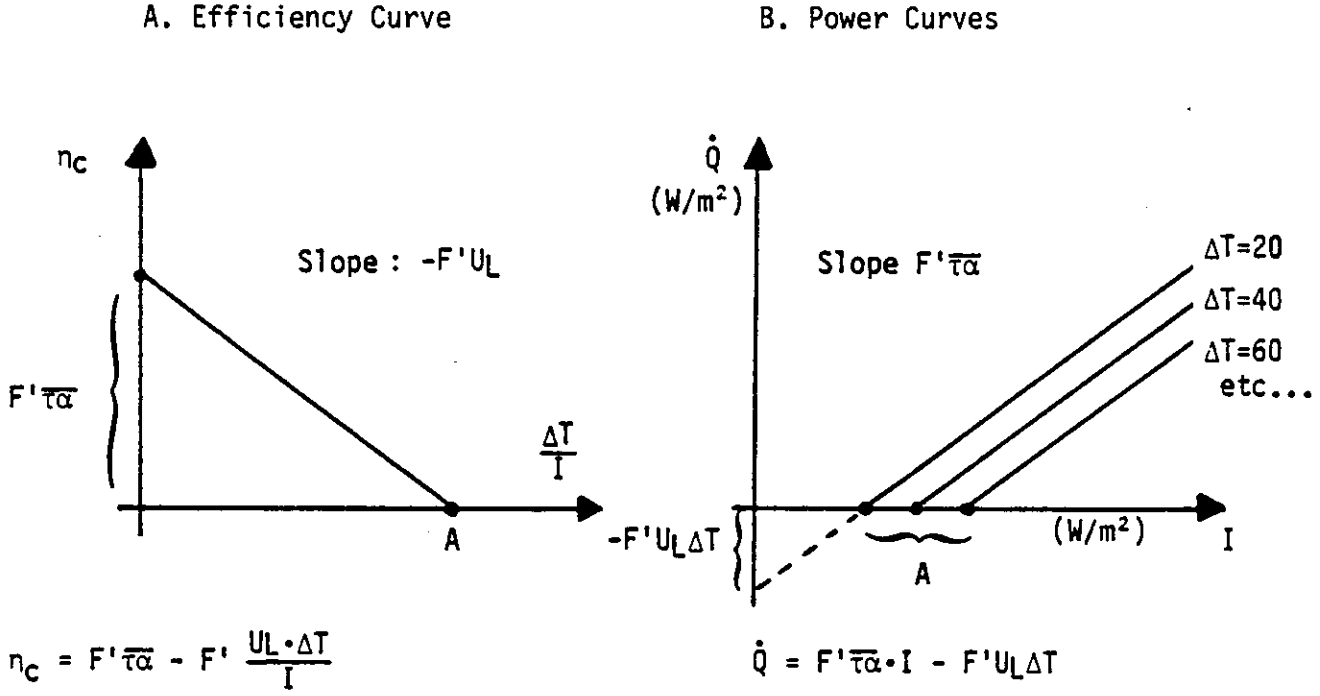

$$\eta_c = F'\overline{\tau\alpha} - F' \frac{U_L \cdot \Delta T}{I}$$

$$\dot{Q} = F'\overline{\tau\alpha} \cdot I - F'U_L\Delta T$$

2.4.1 F' = 1 and no fin effect

$$T_c = T_f \qquad [K]$$

where T_c is the fin base temperature. Now

$$\eta_c = \frac{\dot{Q}}{I} = \overline{\tau\alpha} - \frac{U_L \cdot \Delta T}{I}$$

where $\Delta T = T_f - T_a = T_c - T_a$ [K]

which is schematically equivalent to

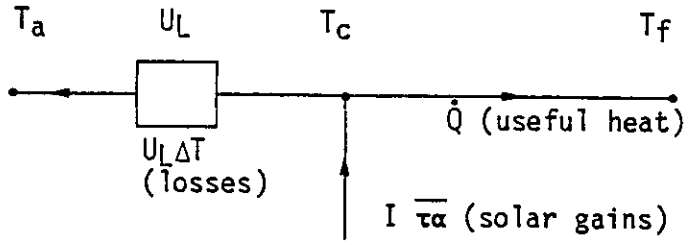

2.4.2 No fin effect, but thermal conductance from fin base to fluid (U_{cf})

U_{cf} may be related to exchange coefficients, conductivity, and/or a heat pipe between absorber and fluid. U_{cf} is also normalized to the reference area.

Then

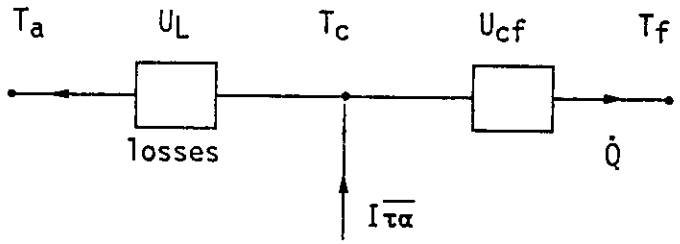

$T_c \neq T_f$

$$\eta_c = \frac{\dot{Q}}{I} = \frac{1/U_L}{1/U_L + 1/U_{cf}} \left(\overline{\tau\alpha} - U_L \frac{\Delta T}{I}\right)$$

where $\Delta T = T_f - T_a$ [K]

which is also equivalent to

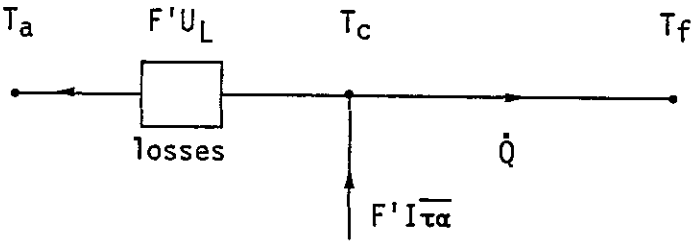

$$n_c = \frac{\dot{Q}}{I} = F'(\overline{\tau\alpha} - U_L \frac{\Delta\bar{T}}{I})$$

with $$F' = \frac{1/U_L}{1/U_L + 1/U_{cf}}$$

2.4.3 Both effects, fin effect and U_{cf}

A careful treatment with temperature varying along the fin leads to the equivalent case

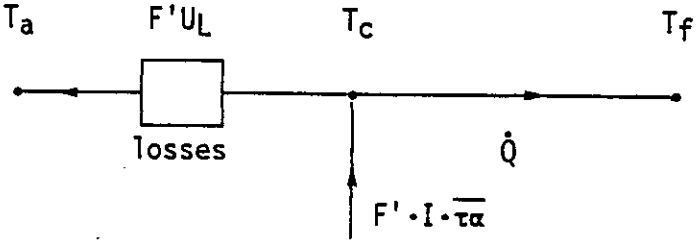

$$n_c = \frac{\dot{Q}}{I} = F'(\overline{\tau\alpha} - U_L \frac{\Delta T}{I})$$

where $\Delta T = T_f - T_a$ [K]

and $$F' = \frac{1/U_L}{1/(U_L \cdot f) + 1/U_{cf}}$$

where f is a factor directly related to the fin efficiency.

This case is also equivalent to

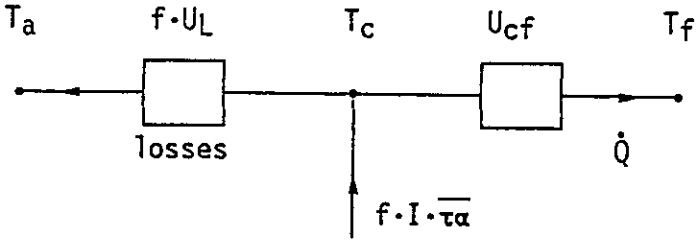

2.5 INSIGHTS FROM IEA-VI EXPERIMENTS

IEA-VI experiments show that the heat conductance between absorber and ambient clearly increases with temperature, and therefore should not be considered temperature independent. Other experimental work also confirms this. Both experiments and theory show that U_L can be written with good accuracy as

$$U_L = K_1 + K_2 \cdot \Delta T_{aba} \qquad [W/m^2 \cdot K]$$

with $\Delta T_{aba} = T_{ab} - T_a$ [K]

where T_{ab} refers to the absorber. If there are no fin effects, then

$T_{ab} = T_c$.

For ETC's, the domination of radiative effects justifies the U_L dependence on temperature difference. The same is no doubt also true for flat plate collectors where the conductance due to convection also depends on temperature.

This temperature dependence, very pronounced at temperature differences around 100 °K, is already significant at medium temperature differences around 50 °K and is highly correlated to the stagnation temperature of a collector at a given solar radiation level. Therefore, stagnation temperature studies, discussed later, complement collector efficiency studies.

Temperature dependence implies a major complication because the corresponding heat loss $U_L \cdot \Delta T_{aba}$ is no longer linear but quadratic in ΔT_{aba}.

In addition to temperature dependence of U_L, we consider the following:

- conductance from fin base to fluid (U_{cf})
- fin efficiency
- incidence angle modifier
  - as related to solar geometry
  - including effects related to the absorber tilt angle (with respect to the collector plane) and
- collector shading.

In the next sections we describe how to deal with these considerations. Of course, we focus on our results and our contributions to ETC characterization, but we feel strongly that such procedures will apply to other collector types.

2.6 COLLECTOR EFFICIENCY WITH QUADRATIC HEAT LOSSES

We will begin with simple cases and then proceed to progressively more complex cases.

2.6.1 Quadratic heat loss dependence and no other effect

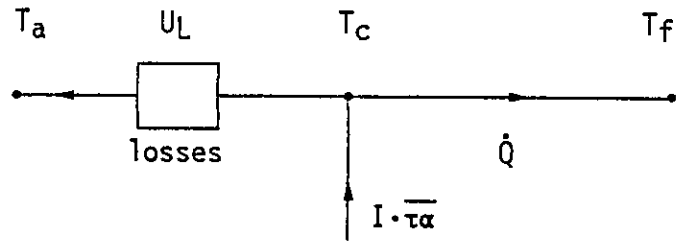

$$T_{ab} = T_c = T_f \qquad [K]$$

$$\Delta T = T_f - T_a \qquad [K]$$

$$U_L = K_1 + K_2 \cdot \Delta T \qquad [W/m^2 \cdot K]$$

$$\eta_c = \overline{\tau\alpha} - U_L \cdot \frac{\Delta T}{I} = \frac{\dot{Q}}{I} = \overline{\tau\alpha} - K_1 \frac{\Delta T}{I} - K_2 \frac{\Delta T^2}{I}$$

The Sanyo and Corning Cortec collectors display this type of behaviour. Figure 2 clearly shows that for the range $\Delta T/I > 0.12$ (i.e. $\Delta T = 120°K$ for $I = 1000\ W/m^2$ or $\Delta T = 12°K$ for $I = 100\ W/m^2$), the efficiency strongly depends on both ΔT and I values, not just on the ratio $\Delta T/I$.

Thus the efficiency curve has to be parameterized in either ΔT or I. An equivalent representation can be given by the power curves, where the lines are still parallel, but no longer equally spaced. See Figure 2.

2.6.2 Quadratic heat dependence, finite conductance from absorber to fluid (U_{cf}), and no other effect.

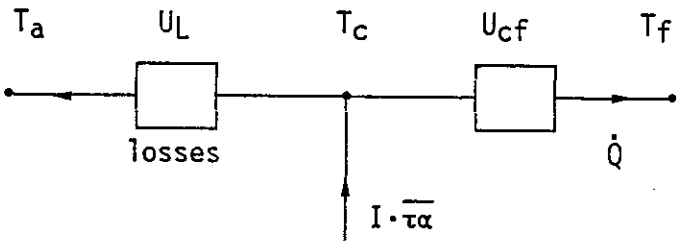

$$\Delta T = T_f - T_a \qquad [K]$$

$$\Delta T_{ca} = T_c - T_a \qquad [K]$$

$$\Delta T_{cf} = T_c - T_f \qquad [K]$$

$$\Delta T = \Delta T_{ca} - \Delta T_{cf} \qquad [K]$$

Figure 2. Corning Cortec "E" Efficiency and Power Curves

a. Efficiency Curves *

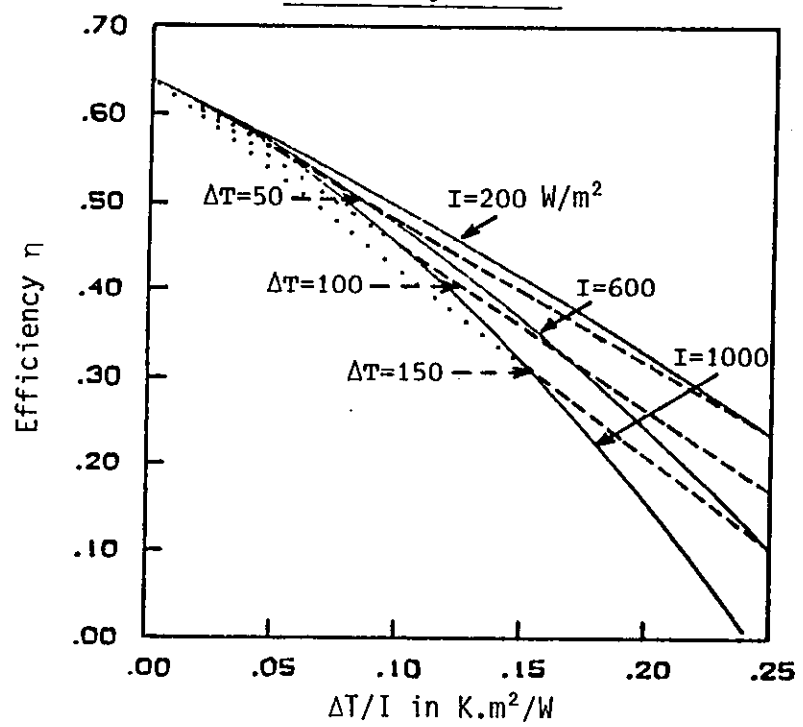

b. Power Curves *

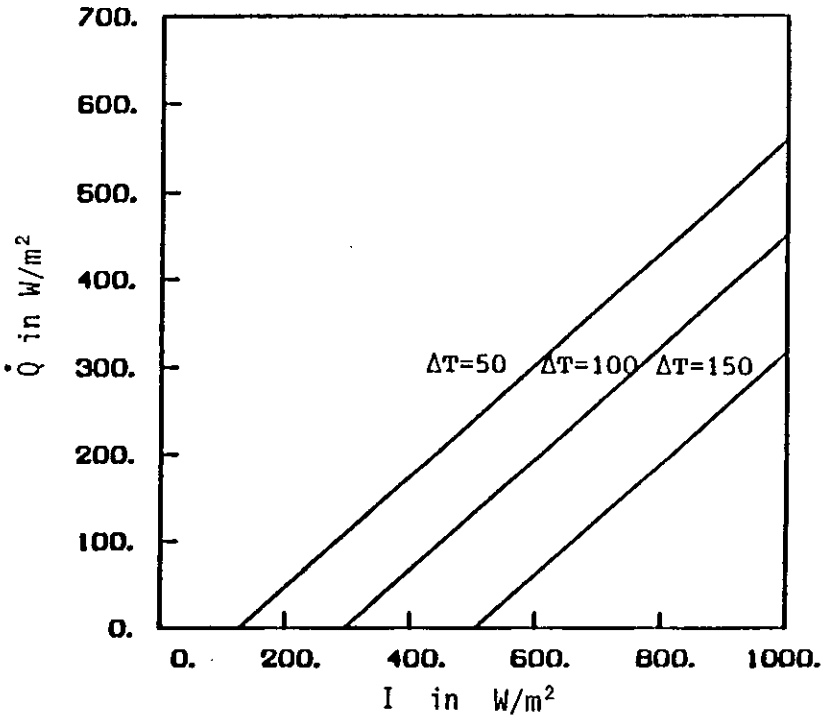

c. Heat Loss Factor *

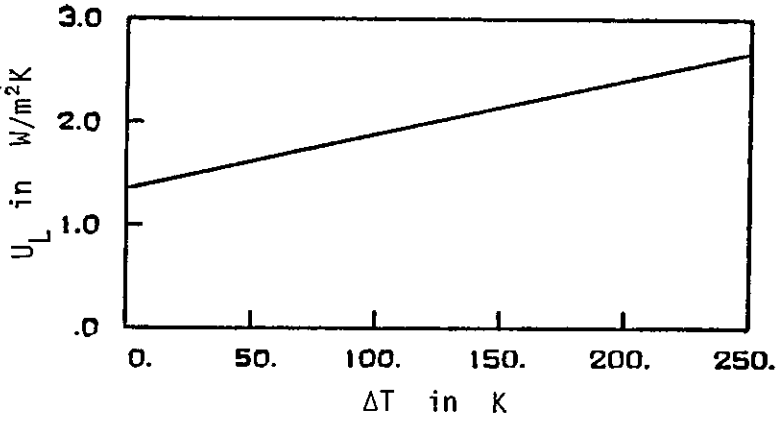

* $\eta = \frac{\dot{Q}}{I} = 0.64 - 1.357 \frac{\Delta T}{I} - 0.0053 \frac{\Delta T^2}{I}$ (units:K,W/m²)

(as deduced from Swiss measurements with conditions : $0 < \Delta T < 250°C$, $I \sim 1000$• W/m²)

$$\dot{Q} = U_{cf} \cdot \Delta T_{cf} \qquad [W/m^2]$$

$$\eta_c = \frac{\dot{Q}}{I} = \overline{\tau\alpha} - U_L \frac{\Delta T_{ca}}{I}$$

$$U_L = K_1 + K_2 \cdot \Delta T_{ca} \qquad [W/m^2 \cdot K]$$

We need to know $\dot{Q}$ or η_c versus the relevant parameters which are ΔT, not ΔT_{ca}, and I.

Using the equation above, eliminating undesired parameters and solving for $\dot{Q}$ versus ΔT and I leads to

$$\dot{Q} = \frac{U_{cf}}{2 \cdot K_2} \left[(-U_{cf} - K_1 - 2 \cdot K_2 \cdot \Delta T) + \sqrt{(K_1 + U_{cf})^2 + 4 \cdot K_2 (U_{cf} \cdot \Delta T + \overline{\tau\alpha} \cdot I)} \right] \qquad (1)$$

where only the positive root is retained. It can be shown that this solution leads to case 2.6.1 if $U_{cf} \to \infty$ and to case 2.4.2 if $K_2 \to 0$.

To eliminate the square root, we can use the approximation

$$\sqrt{1 + x} \cong 1 + \frac{x}{2} - \frac{x^2}{8}$$

which is within one half percent of the exact solution if $x < 0.5$.

ETC's used in Task VI experiments fulfill this condition. Using the approximation we obtain

$$\eta_c = \frac{\dot{Q}}{I} \cong F_U \cdot \overline{\tau\alpha} - F_U^3 \frac{2 \cdot K_2}{U_{cf}} \overline{\tau\alpha} \cdot \Delta T - F_U^3 \frac{K_2}{U_{cf}^2} \overline{\tau\alpha}^2 \cdot I - F_U \cdot K_1 \frac{\Delta T}{I} - F_U^3 \cdot K_2 \frac{\Delta T^2}{I} \qquad (2)$$

where

$$F_U = \frac{1}{1 + (K_1/U_{cf})} = \frac{1/K_1}{1/K_1 + 1/U_{cf}}$$

Expression (2) can be written as

$$\eta_c \cong A - B \cdot \Delta T - C \cdot I - D \cdot \frac{\Delta T}{I} - E \frac{\Delta T^2}{I} \qquad (3)$$

$$\dot{Q} \cong A \cdot I - B \cdot \Delta T \cdot I - C \cdot I^2 - D \cdot \Delta T - E \cdot \Delta T^2 \qquad [W/m^2] \quad (3')$$

$$\dot{Q} \cong a(I \cdot \overline{\tau\alpha}) - b \cdot \Delta T (I \cdot \overline{\tau\alpha}) - c(I \cdot \overline{\tau\alpha})^2 - D \cdot \Delta T - E \cdot \Delta T^2 \qquad [W/m^2] \quad (3'')$$

In (3) and (3') the five parameters A,B,C,D,E are made up of four basic physical quantities, K_1, K_2, U_{cf} and $\overline{\tau\alpha}$. Alternatively, in (3"), $\overline{\tau\alpha}$ and I are always associated and a,b,c,D,E are made up of K_1, K_2 and U_{cf}.

Let us discuss some properties of equations (2) and (3)

- If $K_2 = 0$, equation (2) reduces to case 2.4.2.
- If $U_{cf} = \infty$, equation (2) reduces to case 2.6.1.
- If $I = 0$, for instance during night loss measurements, only the terms D and E contribute to $\dot{Q}$ in (3') and (3"). K_1 and K_2 losses are reduced because of the conductance U_{cf}.
- If $\Delta T=0$, only terms A and C contribute to $\dot{Q}$ in (3') and to η_c in (3). Thus, the efficiency at $\Delta T=0$ depends on I and $\eta_c = A - C \cdot I$. The first 3 terms of equations (2) and (3) show that the optical efficiency depends on ΔT and I. ("Optical" efficiciency is not really the proper term). The last two terms of equations (2) and (3) describe the heat loss dependencies.

In conclusion, equation (3) is consistent with respect to usual cases like 2.4.1 and 2.4.2 and adequately describes the performance of ETC's. The physical meaning is established for all parameters of the equations. Depending on the particular ETC, some parameters may be zero. Therefore, equation (3) provides the correct basis to fit measurements.

Equation (3) can be represented graphically as

- $\eta_c = \eta_c(\Delta T/I)$ for a given I or ΔT on efficiency curves or
- $\dot{Q} = \dot{Q}(I)$ for a given ΔT on power curves. See Figure 2.

Now, we no longer get a straight line for the efficiency curve. Also, the efficiency curve intercept at $\Delta T/I = 0$ depends on I. The power curves are no longer equally spaced for equal ΔT variations. Other similar properties can be easily deduced.

2.7 STAGNATION TEMPERATURES

Efficiency curves are usually developed with low ΔT's. Interpretation of these curves can be enhanced by studying stagnation temperatures.

We measured stagnation temperature T_s by introducing a long and flexible temperature sensor through the collector piping of the absorber of a tube. This procedure is simple, fast, and reliable. The stagnation temperature is then correlated to solar radiation. The relation T_s (I) is a basic tube characteristic as well as a basic collector characteristic.

With ETC's one can reasonably assume that radiation exchanges between absorber and glass cover dominate other heat transfer mechanisms. In steady state and for flat absorbers

$$\overline{\tau\alpha} I = \frac{2A_{abs}}{A_{ap}} \bar{\varepsilon} \sigma (T_s^4 - T_g^4) \qquad [W/m^2] \quad (4)$$

where $\overline{\tau\alpha}$ = optical efficiency normalized to aperture area
A_{abs}/A_{ap} = one-sided absorber to aperture area ratio
$\bar{\varepsilon}$ = effective absorber emittance
σ = $5.67 \cdot 10^{-8}$ = Stefan-Boltzmann constant $[W/m^2K^4]$
T_s = absorber stagnation temperature and $[K]$
T_g = glass temperature. $[K]$

The effective absorber emittance is based on the mean over both absorber sides and on the previous assumptions. $\bar{\varepsilon}$ is a mean emittance depending on the wavelength. $\bar{\varepsilon}$ is the mean value of $\varepsilon(\lambda)$ weighted accordingly to the Planck Spectrum. Therefore $\bar{\varepsilon}$ can depend on temperature.

Since the heat transfer coefficient between glass and environment is much larger than the corresponding radiative heat transfer coefficient between absorber and glass, we may assume that the glass and ambient temperatures are identical, that is $T_g = T_a$. More precisely, we may replace T_g with T_a in equation (4) and include the above mentioned effect in $\bar{\varepsilon}$, which is then called effective emittance. The effect of doing this is almost negligible.

It is assumed that for a given temperature range $\bar{\varepsilon}$ can be considered constant. Equation (4) gives the relation of T_s (I) to other variables. Though not indicated by the functional notation, it involves T_a. When T_s is at or above 200°C, as is the case for most ETC's on clear day conditions, the influence of T_a is relatively small and can be treated as a secondary effect.

From measurements of T_s, T_a and I, and for the same $\overline{\tau\alpha}$, I and A_{abs}/A_{ap}, we can deduce a stagnation temperature T_{sr} normalized to a reference ambient temperature T_{ar} by

$$T_s^4 - T_a^4 = T_{sr}^4 - T_{ar}^4. \qquad [K^4]$$

A reasonable approximation to this is

$$T_{sr} = T_s - (T_a - T_{ar})\,(T_{ar}/T_s)^3 \qquad [K] \quad (5)$$

Therefore, from measurements of T_s, T_a, and I, we can deduce T_{sr} and I.

These results can be compared to the model given by equation (4) when it is applied for T_{sr} and T_{ar}

$$\overline{\tau\alpha}\, I = \frac{2A_{abs}}{A_{ap}}\, \bar{\varepsilon}\, \sigma\, (T_{sr}^4 - T_{ar}^4) \qquad [W/m^2] \quad (4')$$

One measurement of T_s, T_a, and I is enough to evaluate the quantity $\bar{\varepsilon}/\overline{\tau\alpha}$. Equation (4') then provides a relation for $T_{sr}(I)$, as long as $\bar{\varepsilon}$ and $\overline{\tau\alpha}$ can be considered constant.

If $\overline{\tau\alpha}$ is known from other studies, it provides a direct method of evaluation for $\bar{\varepsilon}$ or even $\bar{\varepsilon}(T_s)$. Direct measurements also provide quantification of how $\overline{\tau\alpha}$ varies when changing the background behind a collector, such as using reflectors or white panels, or when changing other optical conditions such as the incidence angle modifier.

The form of $T_s(I)$ must also be consistent with equation (3) for $\eta_c = 0$.

Of course, one could construct more refined models, but in the case of ETC's, relations (4), (5), and (4') are simple and reasonable.

Figure 3. Stagnation Temperature. Corning CORTEC. (Results from Swiss Participants)

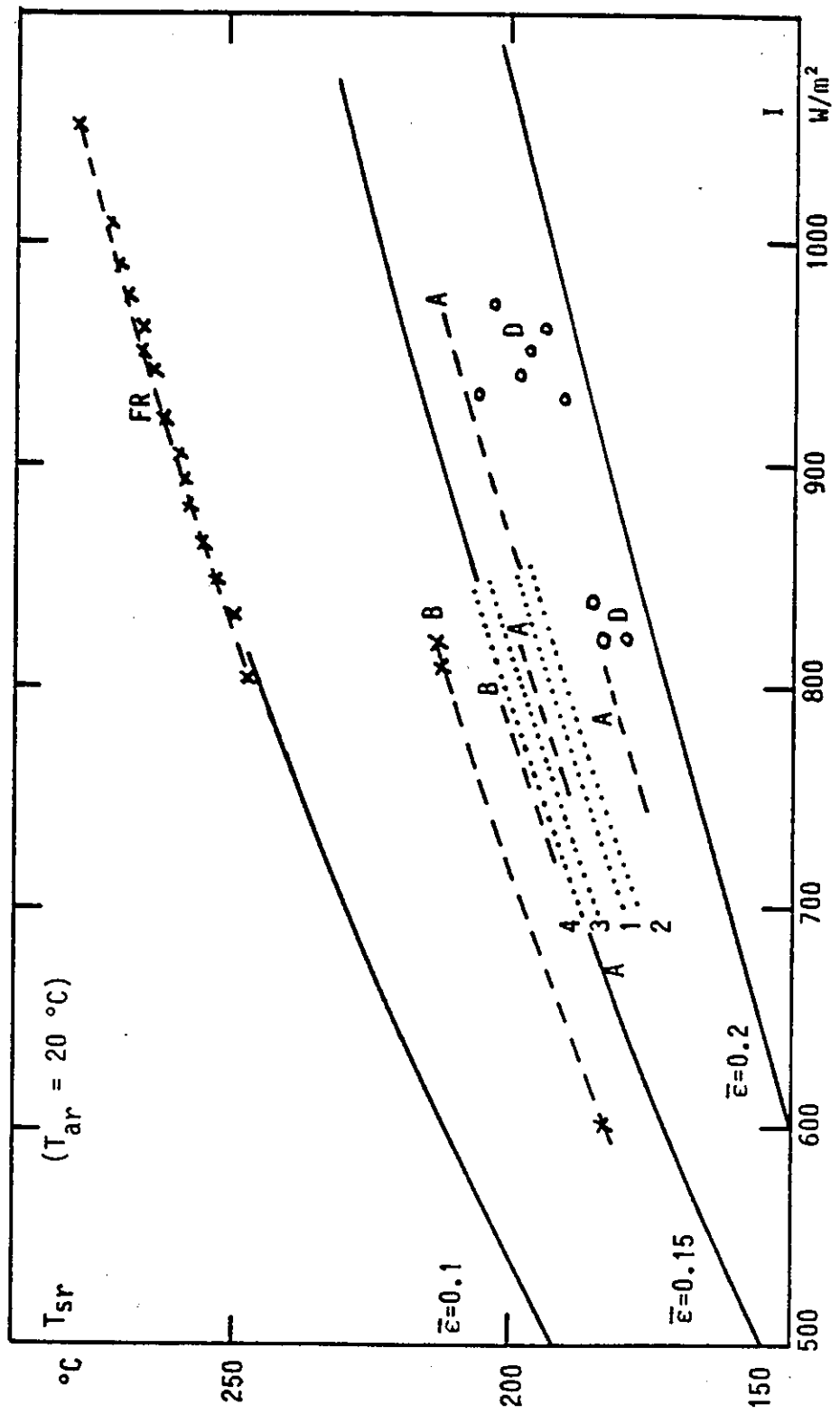

Figure 4. Stagnation Temperature (Results From Swiss Participants)

Measurement of T_{sr} for a sample of 361
Corning CORTEC "E" tubes (T_{ar} = 20°C)
and scattering of T_{sr} after normalization,
according to a simplified model, for I = 800W/m².
See equation (4).

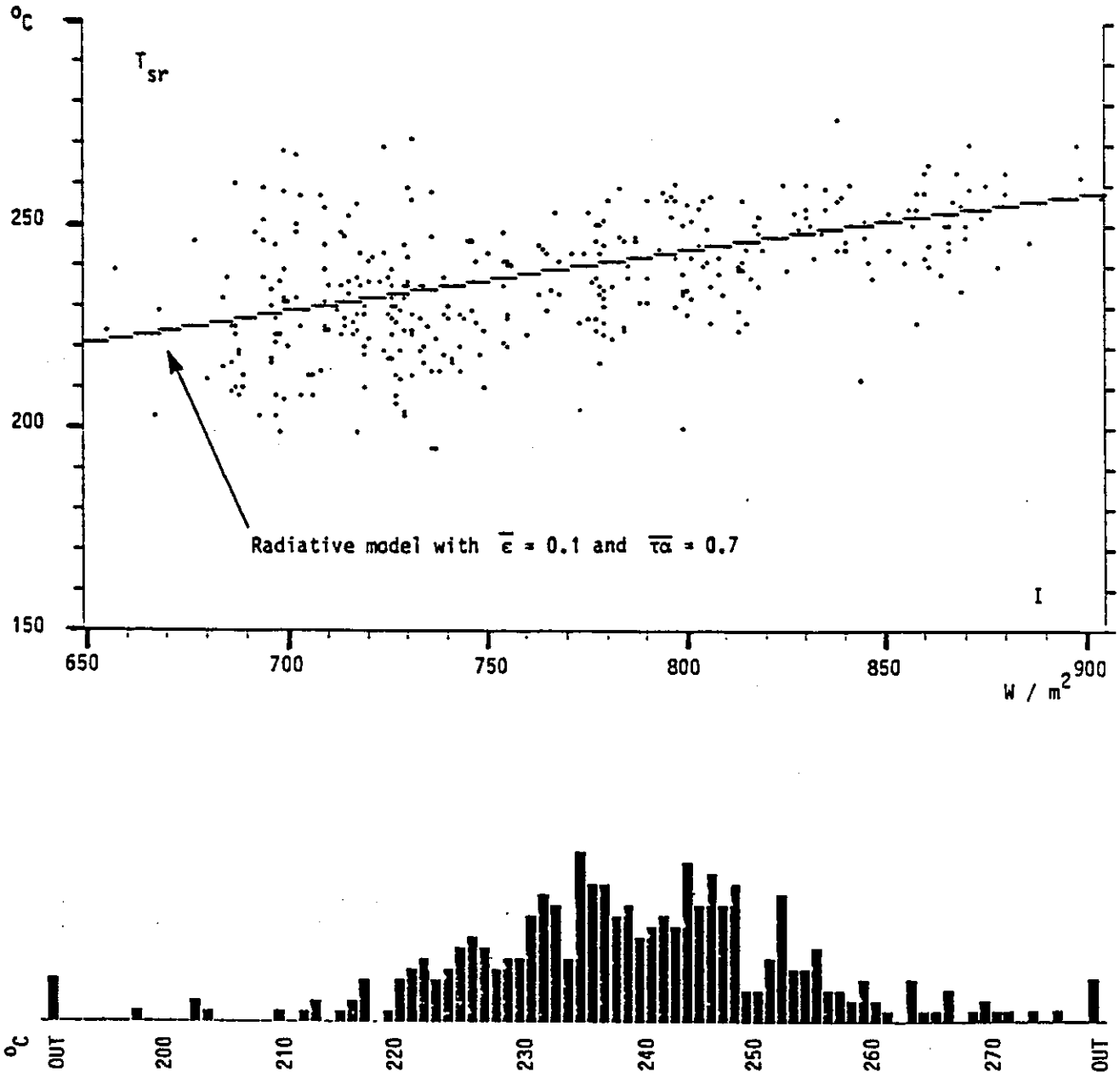

We can now illustrate these considerations:

Figure 3 shows measurements as well as model predictions for earlier Corning CORTEC ETC's. For a limited range of I or T_{sr}, the agreement between the model with $\overline{\varepsilon}$ constant and measurements is satisfactory. Differences in the manufacturing, particularly in the selective coatings, appear clearly. These studies demonstrate the improvement in the selective coating as may be seen in Figure 4 which displays characteristics of the Corning CORTEC E used in the new Swiss installation.

Interesting as well is the scattering of the observed performance for ETC tubes, and consequently for collectors. T_{sr} has a standard deviation of ± 13°K, corresponding to $\overline{\varepsilon}$ ± 0.013. These stagnation temperature models provided a test to allow rejection of a few tubes that performed poorly when mounted.

2.8 FIN EFFECT COMBINED WITH QUADRATIC HEAT LOSSES

Starting with case 2.6.2 and comparing it to case 2.4.3, the fin effect can be introduced by replacing U_L by fU_L and $I\cdot\overline{\tau\alpha}$ by $fI\cdot\overline{\tau\alpha}$ in 2.6.2. But f depends on U_L and, if $U_L=K_1+K_2\Delta T_{ca}$, f depends on T_c or ΔT_{ca}. This is a major complication which did not appear in case 2.4.3 because U_L was a constant, thus allowing an analytical solution. It did not appear in case 2.6.2 where approximations helped to solve a second order equation.

Fortunately, with the ETC's used in Task VI, the fin efficiency is always very close to unity and this problem can usually be avoided.

Consider the following:

- If the temperature does not vary too much along the fin, U_L may be considered constant along the fin; that is, $U_L = U_L(T_c)$, and the same formalism used for case 2.4.3 may be applied.

- It is probably possible to solve the set of equations given for case 2.6.2 iteratively, with $U_L \rightarrow f\cdot U_L$ and $I\cdot\overline{\tau\alpha} \rightarrow fI\cdot\overline{\tau\alpha}$. Assume T_c, compute f, solve the equations, deduce a T_c value, and repeat.

2.9 INCIDENCE ANGLE MODIFIER

When the incident solar radiation is not perpendicular to the collector plane, transmittance and absorptance are modified. Dealing with absorbers tilted with respect to the collector plane also implies other effects that can be included in the incidence angle modifier factor.

This factor, called IAM, is defined as

$$IAM(\gamma,\beta) = \frac{\text{optical efficiency for } (\gamma,\beta)}{\text{optical efficiency for reference conditions}}$$

where (γ,β) refer to the incidence angles γ and β and a given absorber tilt angle, and where the reference conditions are normal incidence and no absorber tilt angle.

This definition should apply only to beam radiation. The IAM factor affects the $\overline{\tau\alpha}$ product in that $\overline{\tau\alpha}$ becomes IAM$\cdot\overline{\tau\alpha}$ in all equations.

For ETC's used in Task VI, incidence angles (γ,β) are defined as shown in Figure 5.

Figure 5. Incidence Angle Definitions

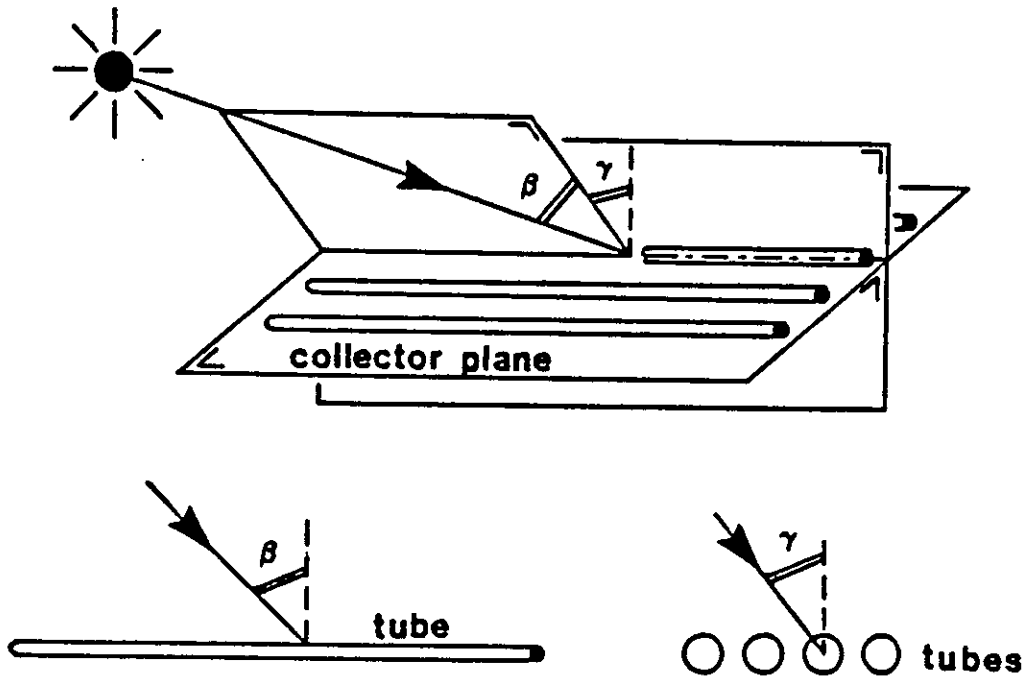

γ = transverse incidence angle
β = axial incidence angle = $\pi/2$ - sun ray to tube axis angle.

In most calculations and measurements, it will be assumed that γ and β dependences are not correlated, that is

$$IAM(\gamma,\beta) = IAM(\gamma) \cdot IAM(\beta)$$

This assumption could be not verified in some cases, reflectors for instance, but none of the IEA Task VI studies have reported such effects.

In this section, we discuss only untilted absorber cases. In the next section we discuss how to introduce absorber tilt angle effects within the incidence angle modifier factor.

According to the definition at normal incidence, IAM(0,0) = 1. As β increases, IAM(β) is expected to decrease in the same way as with flat plate collectors. With flat absorbers, IAM(γ) is expected to remain constant when γ is increased. At large γ values, transmission effects may appear. With cylindrical absorbers, IAM(γ) is expected first to increase, like $1/\cos\gamma$, when γ increases, and then to remain constant due to mutual tube shading. Task-VI experiments seem to verify these expectations.

For the β-dependence, the parametrization used in ASHRAE 93-77 may be used. It is an approximation of the Stokes-Fresnel equations and can be written as

$$IAM(\beta) = 1 - b_o(\frac{1}{\cos\beta} - 1)$$

where b_o is a parameter that can be adjusted to data. See Figure 6.

Although we deal in this chapter only with single ETC characteristics, we include IAM properties as measured from ETC arrays because we strongly feel that they also apply to single ETC's.

How do we evaluate the IAM factors from data ? We first use a given expression for the collector efficiency. Let us take equation (3')

$$\dot{Q} = I \cdot IAM \cdot (A - B \cdot \Delta T) - D \cdot \Delta T - E \cdot \Delta T^2 \qquad [W/m^2]$$

where we temporarily neglect the I^2-term.

By fitting such an expression to data selected for conditions close to normal incidence, we may evaluate the parameters A, B, D and E, where $\dot{Q}$, I and ΔT are given by measurements. Then from other data selected for given (γ,β) values it is possible to extract $IAM(\gamma,\beta)$ for each selected measurement by

$$IAM(\gamma,\beta) = \frac{\dot{Q}+D \cdot \Delta T+E \cdot \Delta T^2}{I(A-B \cdot \Delta T)}$$

where $\dot{Q}$, ΔT and I are measured
and A, B, D and E are from the previous fit.

In other words, we compare the optical efficiency for (γ,β) conditions to the optical efficiency for normal incidence conditions.

This procedure, of course, applies to simpler collector efficiency expressions as well. If the I^2-term has to be taken into account, the same method can be used, but $IAM(\gamma,\beta)$ has to be extracted by solving a second order equation. It is also possible to parameterize $IAM(\gamma,\beta)$, to introduce the corresponding expression within the collector efficiency expression and to evaluate all parameters, including IAM, by a global fit to all data.

So far, we have assumed the solar radiation to be exclusively beam radiation. Let us now deal with a solar radiation including diffuse radiation. Let us define a IAM factor for the diffuse radiation by

$$\overline{IAM} \cdot DIF = \int DIF(\gamma,\beta) \cdot IAM(\gamma,\beta) \cdot d\Omega$$

where DIF = diffuse radiation on collector plane
$DIF(\gamma,\beta)$ = diffuse radiation distribution versus γ and β and
$d\Omega$ = solid angle.

The absorbed solar energy is given by

$$I_a = DIR \cdot \overline{\tau\alpha} \cdot IAM(\gamma,\beta) + DIF \cdot \overline{\tau\alpha} \cdot \overline{IAM}$$

$$I_a = \overline{\tau\alpha} \cdot \underbrace{\left[IAM(\gamma,\beta)\cdot\frac{DIR}{GL} + \overline{IAM}\cdot\frac{DIF}{GL}\right]}_{IAM^*(\gamma,\beta)} \cdot GL$$

where DIR / GL = beam / global radiation on collector plane.

Obviously, now we are facing a major complication. Diffuse and/or beam radiation should be measured as well as the global radiation. Some Task VI participants do it. But even with such measurements, it is not trivial to extract $IAM(\gamma,\beta)$ from $IAM^*(\gamma,\beta)$ and the corresponding data

$$IAM(\gamma,\beta) = IAM^*\cdot\frac{GL}{DIR} - \overline{IAM}\cdot\frac{DIF}{DIR}$$

$IAM^*(\gamma,\beta)$ can be evaluated from data as described before, but $IAM(\gamma,\beta)$ is the relevant quantity. $\overline{IAM}$ involves $IAM(\gamma,\beta)$.

Diffuse radiation may be assumed to be isotropic, a crude approximation, and iterative procedures can be applied in order to get $IAM(\gamma,\beta)$.

We have not gone this far in Task VI studies. Further detailed investigations should be performed along these lines. Nevertheless, interesting features and results have been obtained. They are presented with definitions not yet fully normalized and finalized.

Notice that, if $\overline{IAM}$ is not too different from IAM*, $IAM(\gamma,\beta)$ is close to $IAM^*(\gamma,\beta)$. Some illustrations of the IAM factor are shown in Figures 6,7,8,9 and 10.

Notice also that so far we have neglected effects such as these related to spectral distributions or those induced by differences in evaluation procedures, for instance solar simulator versus outdoor conditions.

2.10 TILTED ABSORBER EFFECTS

When flat absorbers are tilted with respect to the collector module plane, corresponding effects may be taken into account within the partial incidence angle modifier factor $IAM(\gamma)$, that is

$$IAM(\gamma) = IAM_o(\gamma) \cdot TA(\gamma)$$

where the index $_o$ refers to untilted absorber and TA involves tilted absorber effects.

Solar radiation is defined with respect to the collector plane. A lack of solar radiation due to an inadequate collector orientation, a flat roof for instance, may be partly compensated by an increased collector sensivity obtained by tilting the absorbers, so that TA > 1.

Figure 6. Incidence Angle Modifier IAM(β) Parametrization

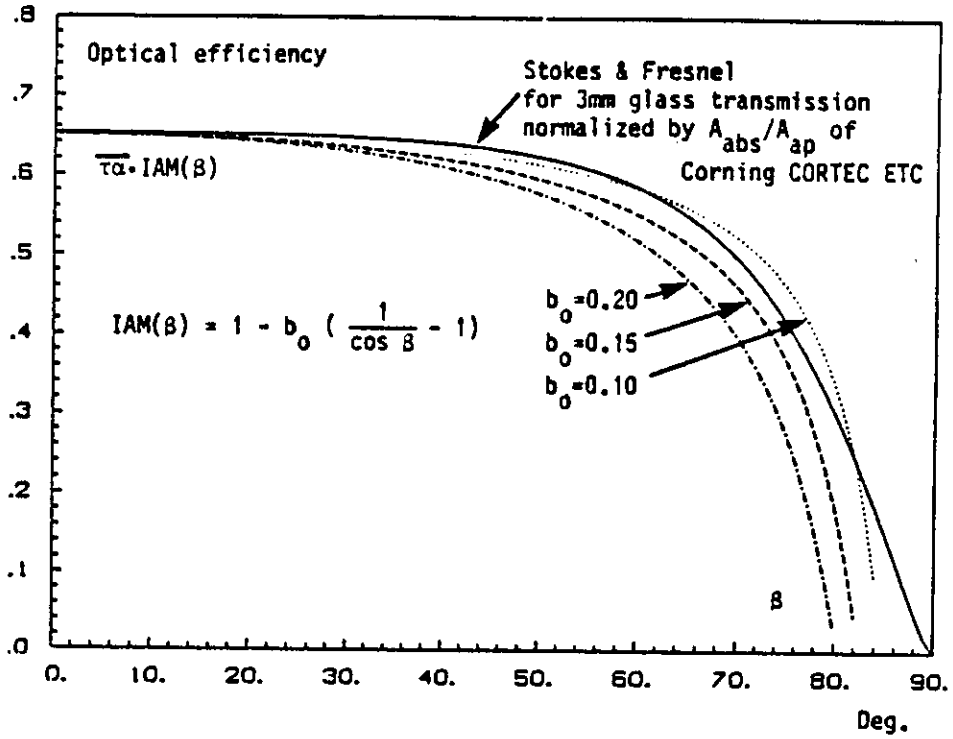

Figure 7. SOLARCAD Corning CORTEC "A" Array Hourly Data Fit

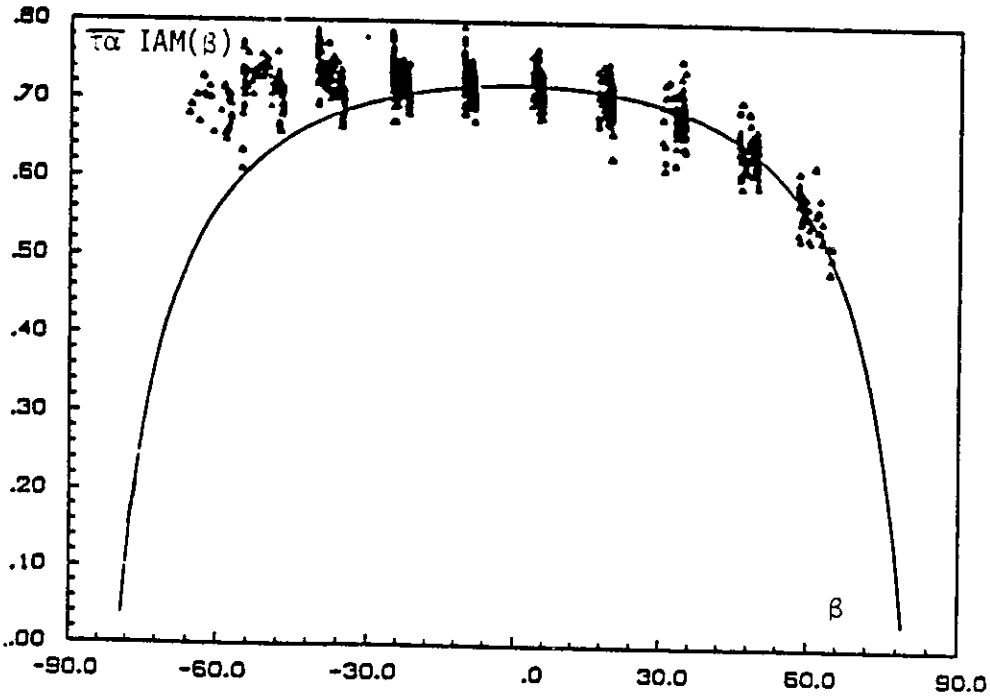

Data points 8a.m.-5p.m. Morning points (β < -30°) behave in an unexpected way. No explanation has been found. b_o is found to be 0.17 in close agreement with SOLARTECH ETC tests (Canada). For a separate evaluation of b_o, see section 2.9.

Figure 8. IAM(γ) for Philips VTR261 ETC at Solar House EUT (NETHERLANDS)

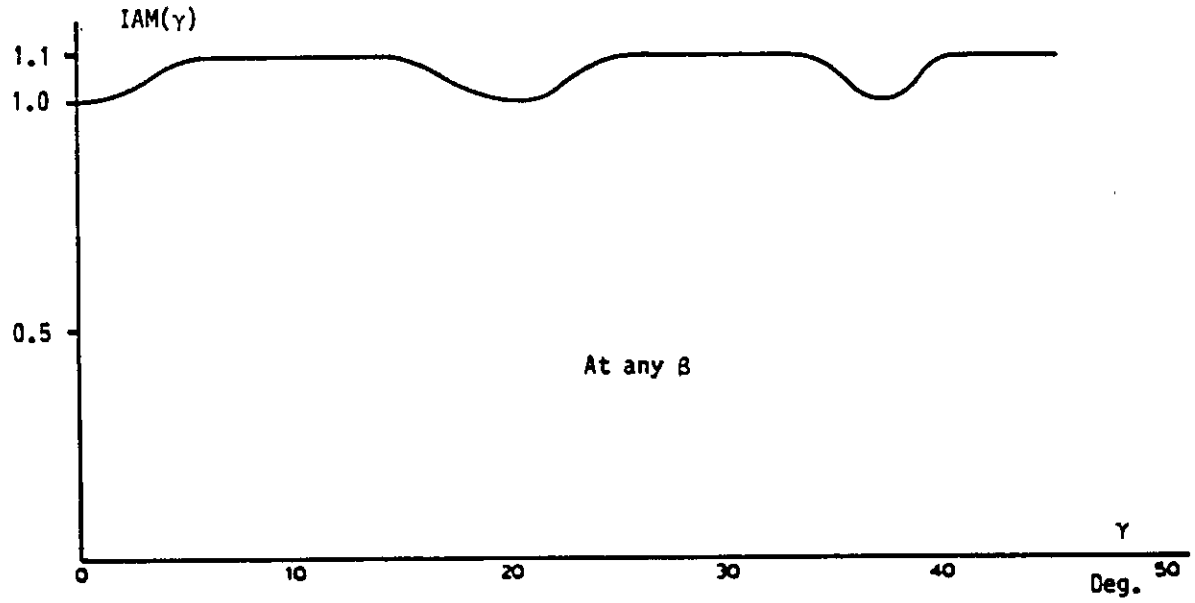

Figure 9. Angular Dependence of Efficiency at Ambient Temperature for the Sydney University ETC.

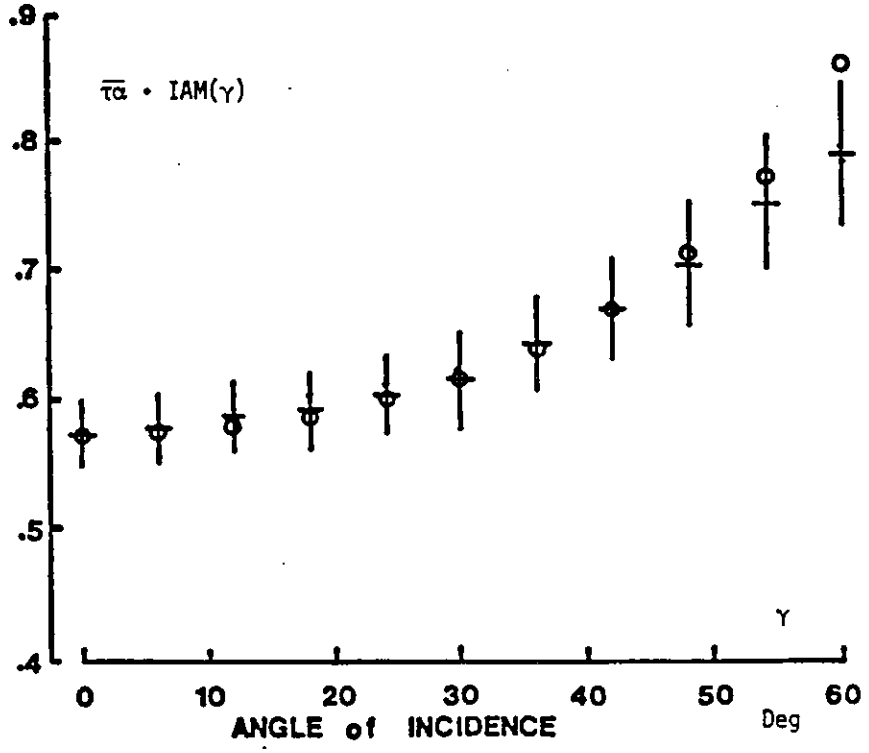

Figure 10. Experimental Determination of the Transmittance Absorbtance Product, as extrapolated from array efficiency data when operating the system at very low $\Delta T/I$ values (test days). The extrapolation is based on results accumulated over long periods.

(Solarhaus Freiburg, F.R.G.)

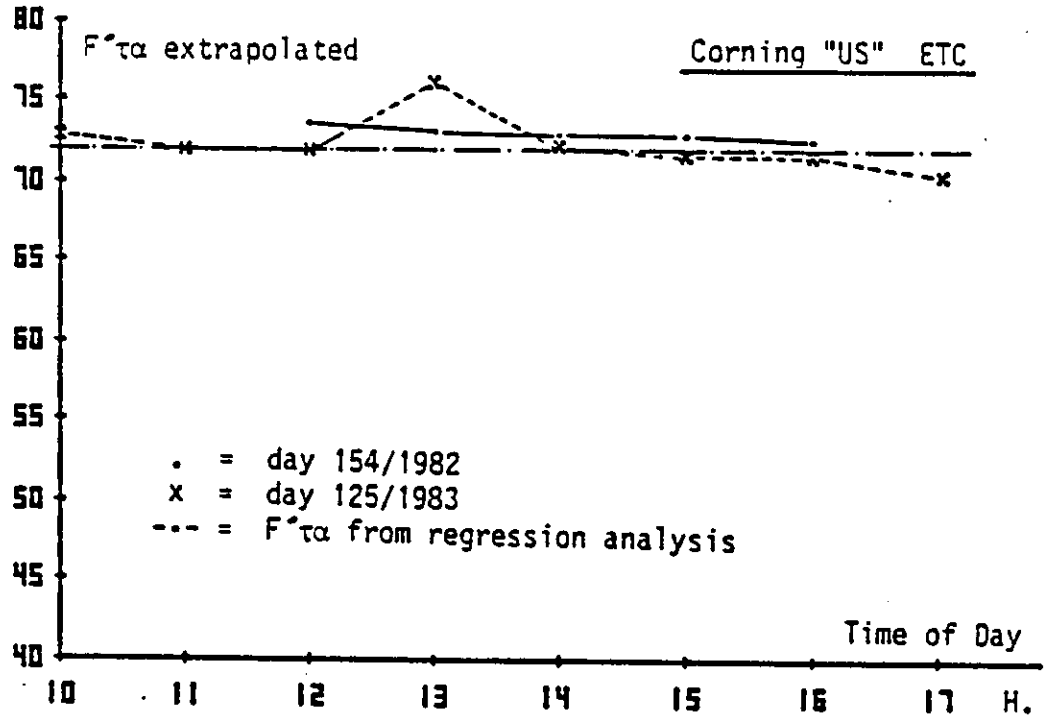

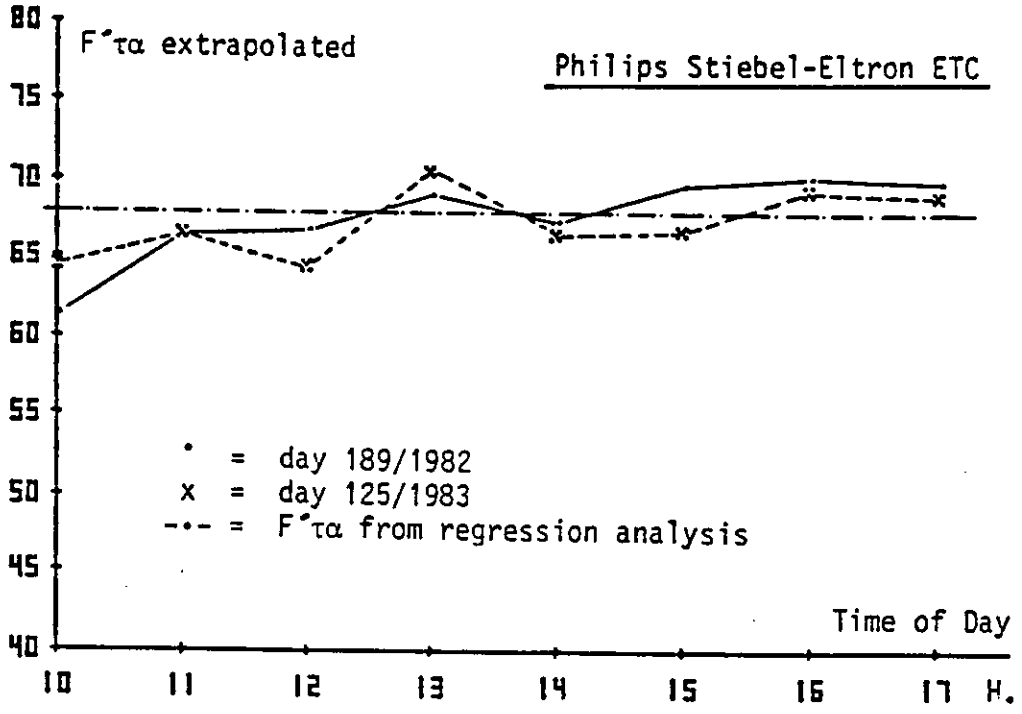

Let us discuss the case of Corning-Cortec in the context of ETC's exposed to pure beam radiation

$$\dot{Q} = \overline{\tau\alpha} \cdot IAM(\gamma,\beta) \cdot I - U_L \cdot \Delta T \qquad [W/m^2]$$

where $IAM(\gamma,\beta) = IAM_o(\gamma) \cdot TA(\gamma) \cdot IAM(\beta) = IAM_o(\gamma,\beta) \cdot TA(\gamma)$

and $U_L = K_1 + K_2 \cdot \Delta T$.

We concentrate now on $TA(\gamma)$. We have, in physical terms

$$\dot{Q} \cdot A_{ap} = \tau\alpha \cdot IAM_o(\gamma,\beta) \cdot A_{abs} \cdot [DIR_{\phi+\theta}(1-SL)] - 2K' \cdot A_{abs} \cdot \Delta T \qquad [W/m^2]$$

where

A_{ap} = aperture area
A_{abs} = absorber area
ϕ = collector plane tilt angle with respect to horizontal
θ = absorber plate tilt angle with respect to collector plane

DIR_ϕ, DIF_ϕ, GL_ϕ } = beam, diffuse, global on collector plane (ϕ)
$DIR_{\phi+\theta}$, $DIF_{\phi+\theta}$, $GL_{\phi+\theta}$ } = or absorber plane ($\phi + \theta$) [W/m²]

γ = axial incidence angle on collector
p, ℓ = pitch of evacuated tubes and single absorber width
K' = heat loss per unit of absorber area
SL = shadow loss factor (from tube to tube)
τ, α = physical transmission and absorption coefficients.
See Figure 11.

Normalizing $\dot{Q}$ to the radiation incident on collector plane, $I=DIR_\phi$, gives the efficiency

$$\eta = \frac{\dot{Q}}{I} = \underbrace{\tau\alpha \cdot \frac{A_{abs}}{A_{ap}}}_{\overline{\tau\alpha}} \cdot IAM_o(\gamma,\beta) \cdot \underbrace{\frac{DIR_{\phi+\theta}\,(1-SL)}{DIR_\phi}}_{TA(\gamma)} - \underbrace{2K' \frac{A_{abs}}{A_{ap}} \cdot \frac{\Delta T}{DIR_\phi}}_{U_L}$$

$\overline{\tau\alpha}$ and U_L correspond to physical properties of the considered ETC's, whatever the absorber tilt angle can be. Absorber tilt angle effects are included only in $TA(\gamma)$.

In order to get $\overline{\tau\alpha}$ and U_L from data, for instance through fits, $\dot{Q}$, ΔT and I (=DIR_ϕ) must be measured, but $TA(\gamma)$ has also to be evaluated. That involves only geometric considerations.

Another interpretation of the previous efficiency expression is:

$$\eta' = \frac{\dot{Q}}{DIR_{eff}} = \overline{\tau\alpha} \cdot IAM_o(\gamma,\beta) - U_L \frac{\Delta T}{DIR_{eff}}$$

where $DIR_{eff} = DIR_{\phi} \cdot TA(\gamma)$ represents the effective solar radiation reaching the absorbers normalized on the collector plane and the aperture area. η' is the usual efficiency for ETC's with untilted absorbers for the case where incident radiation is DIR_{eff}.

Of course, accounting properly for diffuse radiation leads to a rather complex situation.

- As seen before, complications are due to the usual incidence angle modifier effects.
- TA (γ) can be written, as

$$TA(\gamma) = \frac{DIR_{EFF}+DIF_{EFF}}{DIR_{\phi}+DIF_{\phi}} = \frac{GL_{EFF}}{GL_{\phi}}$$

where DIR_{EFF}, DIF_{EFF}, GL_{EFF} correspond to effective radiations reaching the absorbers.

When extracting physical ETC parameters from data, beam and diffuse radiations in the absorber plane have to be evaluated or measured as well as the radiation in the collector plane. We recommend doing it when dealing with test or demonstration systems.

About the beam radiation we have

$$DIR_{EFF} = DIR_{\phi+\theta} (1-SL).$$

The effective diffuse radiation can be measured by use of a shadowing geometry similar to the absorber geometry. If not measured the diffuse radiation involves the use of a model which could simply be

$$DIF_{EFF} = DIF_{\phi}.$$

It was found from solar radiation measurements within the SOLARIN project that $DIF_{\phi+\theta}$ may exceed DIF_{ϕ} by 50%. This effect is attributed to a luminous horizon band which actually is not seen by tilted absorbers (but by solarimeters). Then effectively DIF_{EFF} as seen by absorbers may be close to DIF_{ϕ}. As we see, it is a very complex situation requiring caution.

- Different effects may be correlated.
- Diffuse radiation reaching the absorber back can not be easily evaluated.
- Reflectors, if any, modify significantly radiative properties.

As already mentioned, we restrict ourselves, within IEA Task VI, to identify properly all relevant and significant effects and to provide guide lines for a refined methodology.

As an illustration we show now how to evaluate $TA(\gamma)$ for pure beam radiation in case of the Corning-Cortec ETC. See Figure 11.

We neglect transmission effects through other glass tubes as well as module edge effects. The following considerations are purely geometrical. The transverse incidence angle (γ) depends on ϕ and can be deduced from the knowledge of the sun's motion. Shading (SL) appears for γ values larger than a limit given by

$$\gamma_{lim} = \tan^{-1}\left(\frac{p-\ell\cos\theta}{\ell\sin\theta}\right)$$

The shadowing fraction is given by

$$\gamma \leq \gamma_{lim} \qquad SL = 0$$

$$\gamma > \gamma_{lim} \qquad SL = 1 - \frac{p}{\ell}\left(\frac{1}{\tan\gamma\cdot\sin\theta + \cos\theta}\right)$$

For beam radiation we have:

$$\frac{DIR_{\phi+\theta}}{\cos(\gamma-\theta)} = \frac{DIR_{\phi}}{\cos\gamma} \quad (= \text{unprojected beam radiation})$$

Taking conditions similar to the SOLARIN project leads to

$p = 110mm; \quad \theta = 30°; \quad \ell = 88mm; \quad$ any ϕ.

$\gamma_{lim} = 37.5°$

$$TA(\gamma) = \frac{DIR_{\phi+\theta}}{DIR_{\phi}}(1-SL) = \begin{cases} \dfrac{\cos(\gamma-\theta)}{\cos\gamma} & \gamma \leq \gamma_{lim} \\ p/\ell = 1.25 & \gamma > \gamma_{lim} \end{cases}$$

$TA(\gamma)$ behaves in a remarkably simple way. See Figure 12.

- For $\gamma = 0$, $TA(\gamma) = \cos\theta$.
- For $\gamma < \gamma_{lim}$, tilting the absorber is equivalent to tilting the collector.
- For $\gamma > \gamma_{lim}$, shadow losses reduce the previous compensation. Nevertheless, a 25% gain, as compared to untilted absorber conditions, is achieved.

These considerations may be somewhat affected when considering the diffuse radiation. But as long as only the beam radiation is considered or as long as the diffuse fraction is low, the previous considerations look reasonable.

Figure 11. Tilted Absorber Geometry

Geometry:

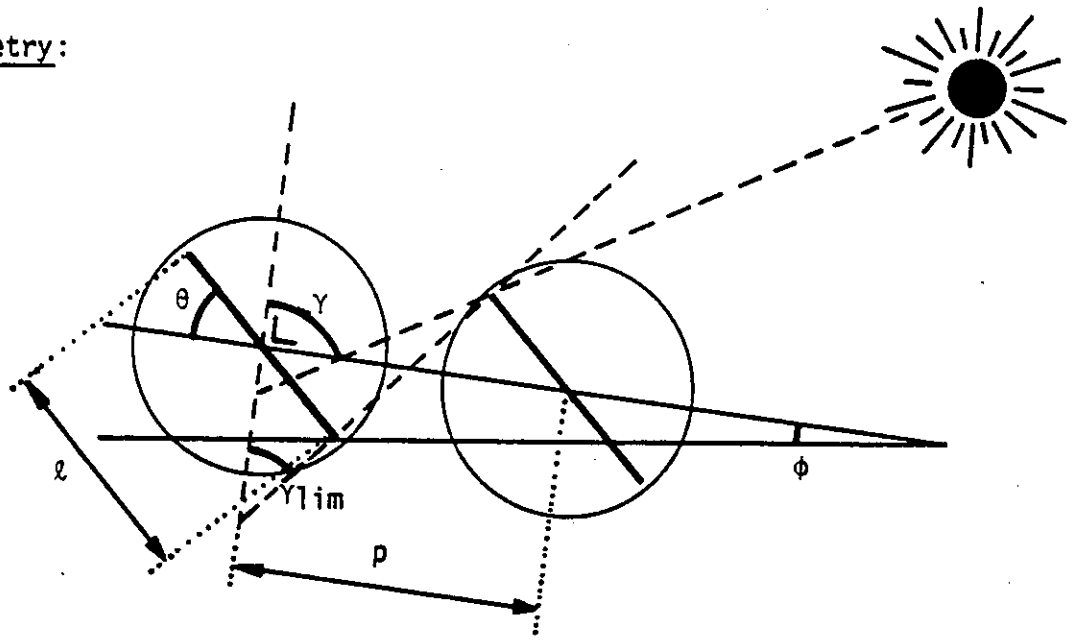

Figure 12. Tilted Absorber Factor.

Corning-Cortec geometry, absorber tilt angle θ = 30°
TA(γ) = absorber tilt angle effect (TA > 1 ⇒ gain)

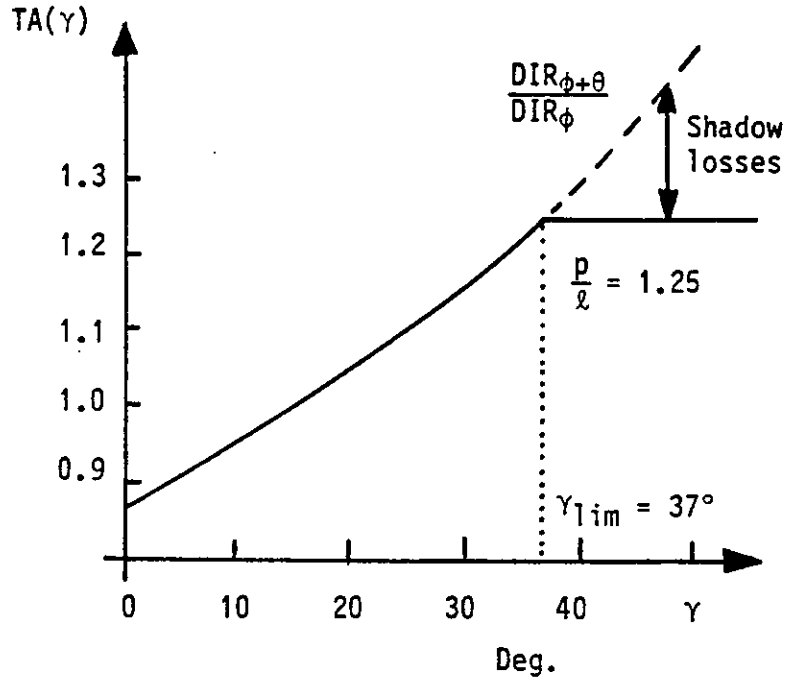

TABLE 2-1. SINGLE COLLECTORS USED IN IEA-VI EXPERIMENTS.
GEOMETRICAL AND DESIGN FEATURES.

COUNTRY	ETC TYPE	NUMBER OF TUBES PER MODULE	PITCH [mm]	LENGTH FOR APERTURE AREA DEFINITION [mm]	APERTURE[2] PER MODULE [m²]	GROSS AREA PER MODULE [m²]	←EXTERNAL GLASS MATERIAL
AUSTRALIA	Sydney University	15	60	1390	1.25	1.47	Borosilicate Glass
CANADA	SOLARTEC[5]	8	152	1055	1.30	1.64	Borosilicate Glass[6]
C.E.C	Philips VTR361[8]	14	104	1560	2.27	2.75	Soda Lime Glass
	Philips VTR261[8]	19	75	1560	2.22	2.75	Soda Lime Glass
	Sanyo STC-CU250L	10	93	2602	2.42	2.77	Soda Lime Glass
F.R.G	Corning "US"	6	113	2140	1.45[9]	≈1.86	Pyrex
	Philips VTR261[8][10]	12	104	1560	1.947	2.41	Soda Lime Glass
NETHERLANDS	Philips VTR261[8]	16	82	1560	2.05	2.57	Soda Lime Glass
SWEDEN	Philips VTR141[8]	19	75	961	1.37	1.80	Soda Lime Glass
	General Electric TC100	8	NIA	NIA	1.37	1.63	Soda Lime Glass
	Owens Illinois Sunpak	24	NIA	NIA	2.55	NIA	Borosilicate Glass
	Teknoterm HT(F.P.)[15]	NA	NA	NA	NIA	0.7	NIA
	Granges Aluminium(F.P.)[15]	NA	NA	NA	NIA	2.12	NIA
	Scandinavian Solar HT(F.P)[15]	NA	NA	NA	12.0	NIA	NIA
SWITZERLAND	Corning CORTEC "A"	6	111.3	2172	1.45	1.86	Pyrex
	Corning CORTEC "B"	6	111.3	2172	1.45	1.86	Pyrex
	Sanyo STC-CU250 L	10	97.2	2524	2.44	2.77	Pyrex
SWITZERLAND	Corning CORTEC "D"	6	111.3	2172	1.45	1.86	Pyrex
SWITZERLAND	Corning CORTEC "E"[12]	6	111.3	2172	1.45	1.86	Pyrex
USA	Philips VTR361[8]	14	104	1560	2.27	2.67	Soda Lime Glass
	Philips VTR141[8]	12	95	1005	1.146	1.68	Soda Lime Glass

Notes : (1) NA for Not Applicable, NIA for No Information Available.
(2) Basic area definition for normalizations. See text (2.1)
(3) Area with selective coating. When flat and selective on both sides, specified as "2•area".
(4) Reflector delivered by the manufacturer as part of the collector.
(5) Equivalent to SUNMASTER DEC 8A.
(6) Kimble KG-33, equivalent to "PYREX" low expansion glass.
(7) Aluminized mylar film bounded to aluminium substrate, reflectivity 0.8, acceptance angle 60°(manufacturer).
(8) The nomenclature of the Philips collectors refers to the tube type, not collector construction.
(9) Experimental results and performance indicators in previous reports are based on an early definition of 1.39m² aperture area per module.

TUBE		ABSORBER				REFLECTOR[4]	
Outside Diameter [mm]	Thickness [mm]	Shape	Tilt angle [deg]	Area per[3] Module [m^2]	Heat Removal	Shape	Material
38	1.4	Cylindrical	NA	1.97	Flow through	Flat	Diffuse white
53	2.0	Cylindrical	NA	1.15	Flow through	CPC	Aluminized Mylar [7]
65.5	1.2	Fin	0°	NIA	Heat pipe	Ripple	Aluminium
65.5	1.2	Fin	0°	NIA	Heat pipe	Flat	Aluminium
80.4	2.1	Fin	0°	NIA	Flow through	Flat	Grey painted steel
100	2.4	Fin	0°	1.12	Flow through	None	
65	1.2	Fin	0°	2·1.092	Heat pipe	Ripple	Aluminium
65	1.2	Fin	0°	2·1.45	Heat pipe	Flat	Tedlar coated aluminium[14]
65	1.2	Fin	0°	NIA	Heat pipe	None	
NIA	NIA	Cylindrical	NA	NIA	Flow through	CPC	Aluminium
NIA	NIA	Cylindrical	NA	NIA	Flow through	CPC	Aluminium
NIA	NIA	NA	0°	NIA	Flow through	NA	
NIA	NIA	NA	0°	NIA	Flow through	NA	
NIA	NIA	NA	0°	NIA	Flow through	NA	
100	2.7	Fin	0°	2·1.12	Flow through	None	
100	2.7	Fin	0°	1.12	Flow through	None	
80	2.0	Fin	0°	2·1.73	Flow through	Flat	White painted sheet[11]
100	2.7	Fin	30°	2·1.12	Flow through	None	
100	2.7	Fin	30°	1.12	Flow through	None	
65	1.2	Fin	0°	2·1.27[13]	Heat pipe	Ripple	Aluminium
65	1.2	Fin	0°	2·0.665	Heat pipe	None	

(10) Philips VTR261 tubes in Stiebel-Eltron modules SOL-50.
(11) In use in the CORTEC "A" array instead of the SANYO array.
(12) New CORTEC collector (improved selective surface) to be installed in the definitive array of 1000m^2 in Geneva SOLARCAD District Heating Project starting at April 1985.
(13) Both sides are coated except for 6.9% of area.
(14) Tedlar coated aluminium film manufactured by Solar Usage Now.
(15) Flat plate collectors

TABLE 2-2. SINGLE COLLECTORS USED IN IEA-VI EXPERIMENTS. CHARACTERISTICS FROM ABSORBER TO COLLECTOR FLUID.

Absorber fluid may be different from collector fluid when dealing with heat pipe.

		← SELECTIVE COATING →					
COUNTRY	ETC Type	MATERIAL	α	ε	SOURCE OF INFORMATION	ABSORBER SUPPORT MATERIAL	THICKNESS [mm]
AUSTRALIA	Sydney University	Copper/graded metal carbide(1)	0.93	0.05(2)	Sydney Univ.	Borosilicate glass	NIA
CANADA	SOLARTEC	Copper chromium oxide	0.8	0.05	Manufacturer	Borosilicate glass	NIA
C.E.C.	Philips VTR361	Cobalt sulfide oxide	NIA	NIA		Steel	NIA
	Philips VTR261	Cobalt sulfide oxide	NIA	NIA		Steel	NIA
	Sanyo STC-CU250L	Nickel base	0.95	0.08	Manufacturer	Copper	NIA
F.R.G.	Corning "US"	Black Chrome	0.95(12)	0.1	Manufacturer	Copper	0.13
	Philips VTR261	Cobalt sulfide oxide	0.95	0.05	Manufacturer	Steel	NIA
NETHERLANDS	Philips VTR261	Black Cobalt	0.92(12)	0.05(7)	Manufacturer	Mild steel	NIA
SWEDEN	Philips VTR141	Cobalt sulfide oxide	NIA	NIA		Steel	NIA
	General Electric TC100	NIA	NIA	NIA		Copper	NIA
	Owens Illinois SUNPAK	NIA	NIA	NIA		Borosilicate glass	NIA
	Teknoterm HT (FP)	Black Chrome	NIA	NIA		Steel	NIA
	Gränges Aluminium (FP)	Aluminium Oxide	NIA	NIA		Aluminium	NIA
	Scandinavian Solar HT(FP)	Aluminium Oxide	NIA	NIA		Aluminium	NIA
SWITZERLAND	Corning CORTEC "A"	Black Chrome	0.95	0.1(8)	Manufacturer	Copper	0.15
	Corning CORTEC "B"	Black Chrome	0.95	0.1(8)	Manufacturer	Copper	0.15
	Sanyo STC-CU250 L	Nickel Base	0.92	0.1	Manufacturer	Copper	NIA
SWITZERLAND	Corning CORTEC "D"	Black Chrome	0.95	0.05	Manufacturer	Copper	0.15
SWITZERLAND	Corning CORTEC "E"	Black Chrome	0.95	0.05(9)	Manufacturer	Copper	0.15
U.S.A.	Philips VTR361	Cobalt sulfide oxide	0.92(12)	0.06(12)	Manufacturer	Copper plated steel	NIA
	Philips VTR141	Cobalt sulfide oxide	0.95	0.03(10)	Manufacturer	Steel	NIA

Notes : (1) dc. reactive sputtered.
(2) $\varepsilon = 0.00012T_s + 0.015$ (T_s = surface temperature in °K): $\varepsilon = 0.05$ at 300°K, 0.06 at 373°K.
(3) Glass tubes are connected on all-copper manifold, consisting of supply, return and support cups, which is an integral part of the collector.
(4) No validity range given. Efficiency data indicate that values apply at least up to 100°C.
(5) Clear sky measurement in Freiburg. T_{amb} = 16°C, T_{glass} = 19°C.
(6) Depends on header pipe material.
(7) Measured at T = 90°C. $\varepsilon = \varepsilon_\perp$.
(8) Stagnation temperature measurements indicate a value of $\varepsilon \simeq 0.17$ at $T_s \simeq 200$°C.

ABSORBER TO FLUID MATERIAL	←HEAT PIPE→ FLUID	CUTOFF TEMPERATURE [°C]	STAGNATION TEMPER. AT 800 W/m² AND 20°C AMBIANT T_{sr}[°C] (11)	←COLLECTOR→ OPERATING PRESSURE (above atm. [bar]	FLUID MAXIMUM PRESSURE pressure) [bar]
Glass + Al fin + Cu U tube	NA	NA	NIA	NIA	NIA
Borosilicate glass tube[3]	NA	NA	350°C[13]	~1	~2
Copper tube	Water	NIA	NA	NIA	NIA
Copper tube	Neopentane	NIA	NA	NIA	NIA
Copper	NA	NA	NIA	NIA	NIA
Copper tube	NA	NA	252±5°C[5]	1	7
Copper tube clamped by Al-block	Neopentane	NIA	NA	NIA	NIA[6]
Al-Copper	Neopentane	NIA	NA	NIA	NIA
Copper tube	Isobutane	160°C	NA	0-1.7	20
Glass + Cu fin + Copper U tube	NA	NA	320°C	2-5	9
Borosilicate glass tube	NA	NA	NIA	NIA	NIA
Steel	NA	NA	200°C	2-5	8
Copper tube	NA	NA	180°C	NIA	25
Copper tube	NA	NA	NIA	NIA	NIA
Copper U tube	NA	NA	~200°C	1	7
Copper U tube	NA	NA		1	7
Copper tube	NA	NA		1	5
Copper U tube	NA	NA		1	7
Copper U tube	NA	NA	242±13°C[9]	1	7
Copper tube	Water	NIA	NA	NIA	NIA
Copper tube	Isobutane	130 °C	NA	1.38	NIA

(9) From measurements on a sample of 360 tubes. (see Fig. 4) T_{stag} value corresponding to $\epsilon = 0.103 \pm 0.013$
(10) May have deteriorated with time.
(11) See text (2.7) for definition of T_{sr}. Measurements at low wind speed.
(12) Given figures apply for air mass 2.
(13) Manufacturer's information for bright sunshine.

TABLE 2-3. SINGLE COLLECTORS USED IN IEA-VI EXPERIMENTS.

THERMAL CAPACITANCE.
Fluid refers to collector fluid, not including heat pipe if any.

COUNTRY	ETC TYPE	FLUID VOLUME IN COLLECTOR [liter/m²]	FLUID CORRESPONDING CAPACITANCE IF WATER C_{CW} [kJ/K•m²]	COLLECTOR EMPTY CAPACITANCE C_{CE} [kJ/K•m²ap]	EXTERNAL GLASS(1) EQUIV.CAPACITANCE C_{CG} [kJ/K•m²ap]
AUSTRALIA	Sydney University	0.875	3.67	7.88	0.45
CANADA	SOLARTEC	8.52	34.9	5.1	insignificant
C.E.C.	Philips VTR361	NIA	NIA	NIA	NIA
	Philips VTR261	NIA	NIA	NIA	NIA
	Sanyo STC-CU250L	0.95	3.99	4.75	0.2 • 6.47
F.R.G.	Corning "US"	0.4(3)	1.67	1.6	0.067 • 10.0
	Philips VTR261	0.14(4)	0.58	4.85	NIA
NETHERLANDS	Philips VTR261	0.2	0.82	3.95	NIA
SWEDEN	Philips VTR141	0.6	2.5	NIA	NIA
	General Electric TC100	0.6	2.5	NIA	NIA
	Owens Illinois Sunpak	11.5	48.0	NIA	NIA
	Teknoterm HT (F.P)	0.8	3.3	NIA	NIA
	Gränges Aluminium(F.P)	0.7	2.9	NIA	NIA
	Scandinavian Solar HT(F.P)	0.8	3.3	NIA	NIA
SWITZERLAND	Corning CORTEC"A"	0.67	2.8	1.5	0.067 • 11.2
	Corning CORTEC"B"	0.67	2.8	1.5	0.067 • 11.2
	Sanyo STC-CU250L	0.94	3.9	3.1	0.095 • 5.6
SWITZERLAND	Corning CORTEC"D"	0.67	2.8	1.5	0.067 • 11.2
SWITZERLAND	Corning CORTEC"E"	0.67	2.8	1.5	0.067 • 11.2
U.S.A.	Philips VTR361	NIA	NIA	4.59	NIA
	Philips VTR141	Negligible	Negligible	0.15(?)	0.33(?)

Notes : (1) According to definitions in section 2.3 : $C_{CG} = {}^{U_C}/_{U_\infty} \cdot C_G$.
(2) Values agree within ± 10% with other published values (manufacturer's, scientific literature).
(3) 30 m of Cu-piping 5mm inner diameter.
(4) 1.32m of Cu-piping 16mm inner diameter.

TOTAL COLLECTOR CAPACITANCE IF WATER $C_C=C_{CW}+C_{CE}+C_{CG}$ [kJ/K·m²ap]	SOURCE OF INFORMATION	VALIDITY
12.0	Components	NIA
40.0	Components[2]	50-100°C
NIA		
NIA		
10.0	Components : JRC ISPRA	
3.94	Components	± 10%
5.57	Components	± 10%
4.77	Components	
16.2	Components	
21.7	Components	
72.0	Components	
40.1	Components	
32.8	Components	
30.0	Components	
5.05	Components	± 20%
5.05	Components	± 20%
7.5	Components	± 20%
5.05	Components	± 10%
5.05	Components	± 10%
4.59	Components	
0.48(?)	Components	

TABLE 2-4. SINGLE COLLECTORS USED IN IEA-VI EXPERIMENTS.
EFFICIENCY CURVE PARAMETERS.

COUNTRY	ETC TYPE	MODEL USED[1]	PARAMETERS F'τα	F'U_L [W/K·m²ap]	OTHERS
AUSTRALIA	Sydney University	$\eta=F'\overline{\tau\alpha}-F'U_L(\Delta T/I)$	0.575	1.74	
		$\eta=F'\overline{\tau\alpha}-F'U_L(\Delta T/I)-B\,\Delta T$	0.575	1.140+0.0064 ΔT	$B=2.78\cdot10^{-4}$ K^{-1}
CANADA	SOLARTEC	$\eta=F'\overline{\tau\alpha}-F'U_L(\Delta T'/I)$[2]	0.455	1.01	
C.E.C.	Philips VTR361	$\eta=F'\overline{\tau\alpha}-F'U_L(\Delta T/I)$	0.64	1.37	
	Philips VTR261	id.	0.65	1.5	
	Sanyo STC-CU250L	id.	0.68	2.1	
F.R.G.	Corning "US"[3]		NIA	NIA	
	Philips VTR261[3]		NIA	NIA	
NETHERLANDS	Philips VTR261	$\eta=F'\overline{\tau\alpha}-F'U_L(\Delta T/I)$	0.68[4]	1.2	
SWEDEN	Philips VTR141	$\eta=F'\overline{\tau\alpha}-F'U_L(\Delta T/I)$	0.62	1.84	
	General Electric TC100		0.60	1.41	
	Owens Illinois SUNPACK		0.65	1.12	
	Teknoterm HT (F.P)		0.70	4.2	
	Gränges Aluminium (F.P)		0.79	3.5	
	Scandinavian Solar HT(F.P)		0.71	3.5	
SWITZERLAND	Corning CORTEC"A"	$\eta=F'\overline{\tau\alpha}-F'U_L(\Delta T/I)$	0.74	1.8+0.015 ΔT	
	Corning CORTEC"B"		NIA		
	Sanyo STC-CU250	id.	0.65	1.3+0.017 ΔT	
SWITZERLAND	Corning CORTEC"D"		NIA		
SWITZERLAND	Corning CORTEC "E"	id.	0.64	1.357+0.0053 ΔT	
U.S.A.	Philips VTR361	$\eta=F'\overline{\tau\alpha}-F'U_L(\Delta T/I)$	0.66	NIA	
	Philips VTR141	id.	0.61	1.8	

Notes : (1) See test, sections 2.4 and 2.6 for definitions.
(2) ΔT' = Inlet - Ambiant temperature.
(3) No measurements of individual modules available.
(4) Low value, due to inadequate spectrum.

SOURCE OF INFORMATION	TEST CONDITIONS/VALIDITY
Own tests	Solar radiation 850<I<1050 W/m² 0<ΔT<150°C Tracking, stationary conditions, 10% diffuse
National Solar Test Facility, CANADA	Solar simulator, 150kW argon arc lamp, 250, 500, 750, 1000 W/m² Each with ΔT=5,30,55,80K. Ambient temperature = 20 °C Flowrate ∿2-the normal value.
JRC-ISPRA	Tests of JRC-ISPRA: Solar radiation, I>600W/m² 0<ΔT<75k Quasi steady state conditions
Manufacturer JRC-ISPRA	
Manufacturer	Solar simulator. Radiation low pressure Xenon. I=500W/m² Perpendicular, 50% diffuse, stationary conditions.
Manufacturer	NIA
Studsvik	Solar radiation, I > 600W/m², steady state
Studsvik	id.
Manufacturer	NIA
Manufacturer	NIA
Standard Test SP Boras,Sweden	NIA
EPFL Lausanne(Switzerland)	Solar radiation 950<I<1000W/m² 0<ΔT<250k Stationary conditions, white painted background
EPFL Lausanne(Switzerland)	As above.
EPFL Lausanne(Switzerland)	As above. No background, no tilted absorber.
Manufacturer	NIA
Manufacturer	Solar simulator (45% diffuse)

TABLE 2-5. SINGLE COLLECTORS USED IN IEA-VI EXPERIMENTS.
INCIDENCE ANGLE MODIFIER. ESTIMATES AND MEASUREMENTS.

COUNTRY	INSTALLATION	ETC-TYPE	IAM(γ, β = 0)[1] 0°	15°	30°	45°	60°	IAM(γ = 0, β)[1] 0°	15°	30°	45°	60°
AUSTRALIA	Sydney University	Sydney University	1.0	1.03	1.08	1.20	1.38	Considered insignificant (simulations only)				
CANADA	Mountain Springs	SOLARTEC	1.0	-	1.15	1.12	0.85	1.0	0.99	0.97	0.92	0.80
			1.0	1.05	1.16	1.31	1.42[4]	Considered insignificant				
F.R.G.	Solarhaus Freiburg	Corning "US"	NIA					Considered insignificant				
		Philips VTR261	Considered insignificant					NIA				
NETHERLANDS	Eindhoven University	Philips VTR261	Between 1 and 1.1(see fig.6.3)					NIA				
SWEDEN		Philips VTR141	Near 1.0					1.0	0.99	0.98	0.94	0.80
		General Electric TC100	1.0	0.94	0.81	0.69	0.68	1.0	0.99	0.98	0.94	0.80
		Owens Illinois SUNPAK	1.0	0.91	0.83	0.82	0.86	1.0	0.99	0.98	0.94	0.80
		Teknoterm HT(F.P)	1.0	0.99	0.98	0.94	0.80	1.0	0.99	0.98	0.94	0.80
		Gränges Aluminium (F.P)	1.0	0.99	0.98	0.94	0.80	1.0	0.99	0.98	0.94	0.80
		Scandinavian Solar HT(F.P)	1.0	0.99	0.98	0.94	0.80	1.0	0.99	0.98	0.94	0.80
SWITZERLAND	Solarcad District	Corning CORTEC "A"	Considered insignificant (∿1.0)					1.0	0.99	0.97	0.91	0.79
		Corning CORTEC "B"	Considered insignificant (∿1.0)					1.0	0.99	0.96	0.89	0.73
		Sanyo STC-CU250L	Considered insignificant (∿1.0)					1.0	0.99	0.97	0.91	0.79
		Corning CORTEC "E"	0.87	1.0	1.15	1.25	1.25	As CORTEC "A"				
SWITZERLAND	Solarin Industry	Corning CORTEC "D"	0.87	1.0	1.15	1.25	1.25	As CORTEC "A"				
U.S.A.	CSU Solar House I	Philips VTR361	1.0	0.99	0.98	1.00	0.99	NIA				
		Philips VTR141	NIA					NIA				

Notes : (1) (γ, β) parameters are γ = Transversal incidence angle β = axial incidence angle (see section 2.9)
(2) Where f_d = diffuse fraction. IAM(γ) does not apply to diffuse, which is considered to have an optical efficiency 0.04 higher than normally incident beam (ray tracing simulation).
(3) Approximation to Stokes-Fresnel laws for flat plate transmission: $IAM(\beta) = 1 - b_o \left(\frac{1}{\cos\beta} - 1\right)$
(4) High IAM values at 45° and 60° may indicate that all transient phenomena have not been fully accounted for yet.
(5) AHD = extracted from array hourly data (IEA-VI).
(6) See also Fig. 7 .

PARAMETRIZATION

$IAM \cdot \overline{\tau\alpha} = 0.611\ f_d + 0.571(1-f_d) \cdot IAM(\gamma)$ (2)	Own tests	Measurements on single panel (1000W/m², low diffuse). Simulation(ray-tracing) in reasonable agreement.
(3)with b_o=0.198	National Solar Test Facility,Canada. Own test AHD[5]	Measurements on single panel at solar simulator. (direct beam 890, 770, 640 and 460 W/m²) $IAM(\gamma)$ evaluated from $IAM(\gamma) = \frac{\eta(\gamma)+F'U_L(\Delta T/I(\gamma))}{\eta(0)+F'U_L(\Delta T/I(0))}$ n values for efficiency corrected for capacitance and array piping heat loss
	AHD	See Fig. 10.
	Manufacturer	Theoretical simulations + estimates
	Boeing report Boeing report	All $IAM(\gamma = 0, \beta)$ are assumed to be near those for flat plate collectors (see Duffie and Beckman)
(3)with b_o=0.21[6]	Own tests	Global fit on hourly data : $\frac{Q112}{H100} = \overline{\tau\alpha}\ IAM(\beta) - (K_1+K_2\Delta T)\frac{\Delta T}{G00T} - C100\frac{ST}{H00T}$ (3)
(3)with b_o=0.27	AHD	No distinction between beam and diffuse components.
(3)with b_o=0.21		
$\gamma<\gamma_{\ell im}$ $IAM(\gamma)=\frac{\cos(\gamma-\theta)}{\cos\gamma}$		Absorber tilt angle effects computed from geometrical considerations. $IAM(\gamma) = TA(\gamma)$. See sect. 2.9 and 2.10.
$\gamma>\gamma_{\ell im}$ $IAM(\gamma)=\frac{\rho}{\ell}$		
		NIA
		NIA

3. ETC ARRAY CHARACTERISTICS

In this section we describe ETC arrays involved in IEA Task VI experiments and determine characteristics based on hourly data recorded over long periods. We recall that an ETC array includes all components (ETC, piping, and other components) between two temperature sensors corresponding to the array inlet and outlet. An array involves only one type of collector.

Following definitions are used by Task VI participants:

T001	[K]	Dry bulb ambiant temperature
T101	[K]	Array inlet temperature
T102	[K]	Array outlet temperature
T100=1/2(T101+T102)	[K]	Mean array fluid temperature
A100	[m²]	Array aperture area
G001	[W/m²]	Solar radiation on collector plane
H001	[MJ/m²]	Solar energy on collector plane (per m²)
H100=H001·A100	[MJ]	Solar energy on collector plane (whole array)
Q112	[MJ]	Heat output from array. $Q112 = W \cdot C_v \cdot (T102 - T101)$ where W = flow rate and C_v = fluid specific heat.

Tables 3-1 through 3-4 displaying array characteristics are given at the end of this section. We now indicate how to derive some of these characteristics.

3.1 SPECIAL MEASUREMENTS ON ETC ARRAYS

An ETC array is a chain of elements. This analysis may be extended to the collection subsystem. The following considerations apply to ETC array components, but they may apply also to other components of the collection subsystem.

The thermal diagram of a given component i, again defined by 2 temperature sensors corresponds to

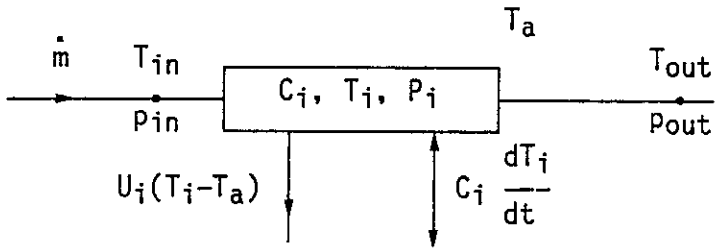

where

T_i	= ½(T_{in} + T_{out}) = mean fluid, or component, temperature	[K]
T_a	= ambient temperature	[K]
p_{in}, p_{out}	= inlet, outlet fluid pressure	[N/m²]
U_i, C_i	= heat loss, thermal capacity (including fluid) for component i	[W/K, J/K]
P_i	= $\dot{V}(p_{in}-p_{out})$ = mechanical pump power dissipated in component i	[W]
$\dot{V}$, $\dot{m}$	= volumic, mass flow rate	[m³/s, kg/s]
c	= fluid specific heat.	[J/kg·K]

Energy balance gives:

$$U_i(T_i-T_a) + C_i \frac{dT_i}{dt} = \dot{m}c\ (T_{in} - T_{out}) + P_i$$

The monitoring system may be used for proper component evaluations. Also useful are pressure gauges. They provide the information necessary for the determination of the mechanical power induced by a pump. Measuring as well the electrical power to the pump gives the pump efficiency, the mechanical to electrical power ratio. For instance, we found in the SOLARCAD experiment a surprisingly low efficiency of 6%, due to design oversizing.

The energy balance expression suggests different experiments:

- To get rid of the solar radiation influence, measurements are performed by night. The solar loop is heated and kept at roughly constant temperature by using heat from storage or auxiliary energy. Therefore, in stationary conditions

$$\left(\frac{dT_i}{dt} = 0\right)$$

$$U_i = \frac{\dot{m}c(T_{in}-T_{out}) + P_i}{T_i-T_a}$$

- We then stop heating the solar loop. We keep the pump running. The temperature decreases at a quasi exponential decay and we get knowing U_i from previous measurements

$$C_i = [\dot{m}c\ (T_{in}-T_{out}) + P_i - U_i(T_i-T_a)] \cdot \left(\frac{dT_i}{dt}\right)^{-1}$$

For these tests, sequential measurements are taken using the usual data acquisition system to improve accuracy. Numerical smoothing may help in order to get relevant results for very small temperature differences. Notice that if the condition $dT_i/dt = 0$ is not fully achieved when evaluating U_i, capacity corrections can be applied in a recurrent way.

Performing this test on the Swiss SOLARIN project showed that the heat loss factor for the ETC array depends on temperature. Assuming this factor to be dominated by radiative losses from absorber to glass gives

$$U_{array} = 8\,\bar{\varepsilon}\ \frac{A_{abs}}{A_{ap}}\ \sigma\ \bar{T}^3 \qquad [W/m^2\cdot K]$$

where $\bar{\varepsilon}$ = equivalent emissivity (for both absorber sides)
A_{abs}, A_{ap} = absorber, aperture area
σ = Stefan-Boltzmann constant
$\bar{T}$ = $\frac{1}{2}(T_{abs} + T_a)$
T_{abs} = absorber (fluid) temperature
T_a = ambient temperature

At $\bar{T}$ = 40°C, the measured value U_{array} = 1.77W/m²·K would yield $\bar{\varepsilon}$ = 0.164 which is in good agreement with other measurements of stagnation temperatures for single modules.

Figure 13 shows some results of this experiment. The fit through the data is in good agreement with the above radiation model, especially for the slope of the curve which characterizes the temperature dependence of the array heat loss factor.

Actually, the array heat loss factor determined by night measurement is found to be smaller than in operational conditions with solar radiation, due to the reverse temperature gradient in the absorber fin.

Figure 13. Night Measurements of the Array Heat Loss Factor for the Swiss SOLARIN Experiment.

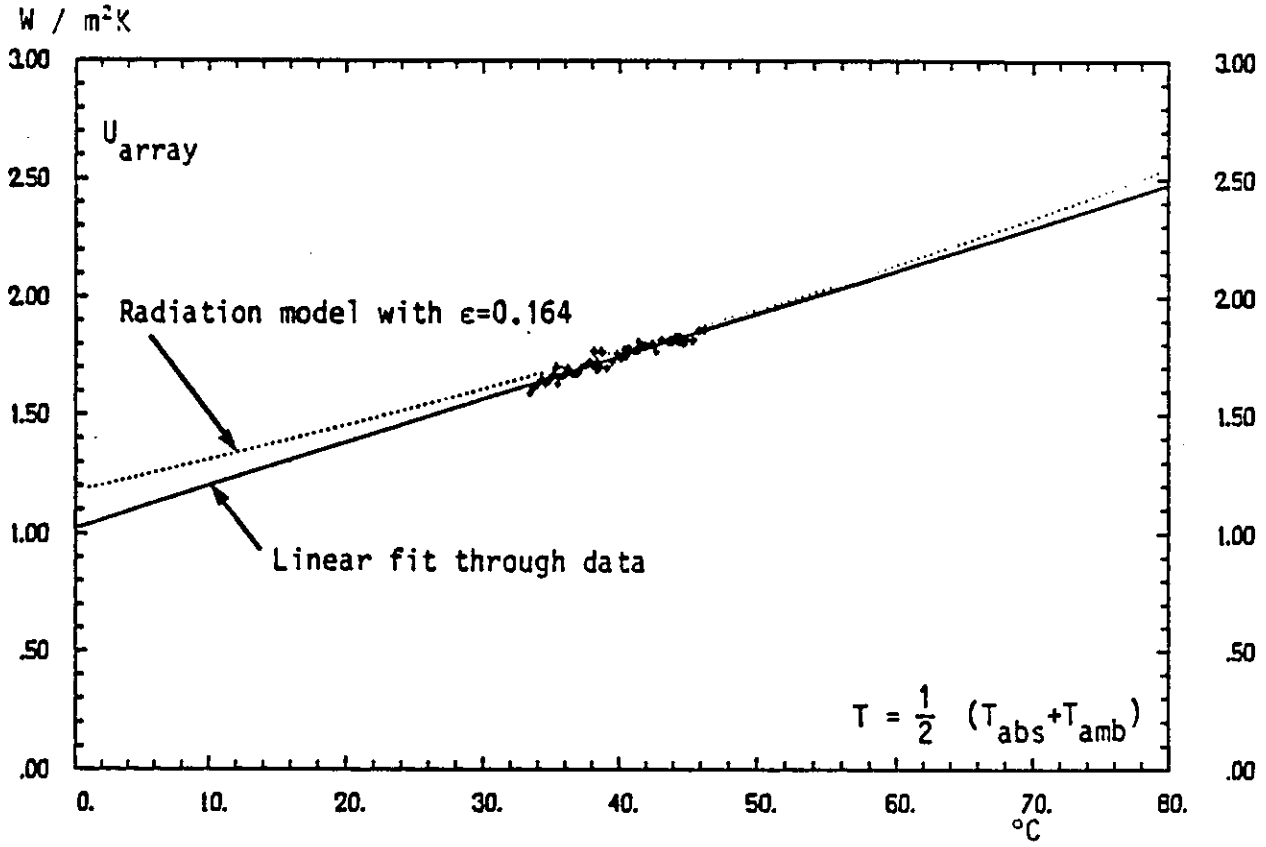

3.2 ETC ARRAY CHARACTERISTICS FROM HOURLY DATA

Although hourly array efficiencies, as measured by IEA Task VI participants, seem to be very similar to instantaneous efficiency curves for single collector modules, they are somewhat different and provide a powerful information in many respects:

- Recorded over long periods, they account for a lot of realistic dynamic conditions such as solar radiation changes, diffuse fraction, beam radiation angles, ambient and user temperatures, wind, snow.
- They include additional heat loss and thermal capacity effects such as piping, other components.
- They correspond to mean values for a sample of modules whose characteristics are not always identical.
- They show medium or long term performance evolution.

To get relevant characteristics and to allow comparisons hourly data are required to fulfil given conditions:

- Hourly data must correspond to continuous array operation.
- Hourly data are restricted to the period 11a.m. - 2p.m., solar time.
- The array heat output Q112 is corrected for thermal capacity

$$Q105 = (T100_n - T100_{n-1}) \cdot C100 \qquad [MJ]$$

where C100 is the thermal capacity between T101 and T102 and where n-1 and n refer to the beginning and the end of the measurement period.

Array efficiency expressions are then fit to the data, and characteristics are extracted.

For simplicity we choose array efficiency expressions similar to single ETC efficiency expressions. However component parameters (like heat loss factor or thermal capacity for single ETC's, piping, other components) do not simply add to each other in all cases to give the corresponding array parameter. Additivity may be the case or roughly the case in many instances, but careful investigations are still needed. The purpose of modeling is to combine component characteristics to get global characteristics. Validation should justify the procedure. Within IEA Task VI we evaluate global array characteristics.

Standard parameters, $F'\overline{\tau\alpha}$ and $F'U_L$, are estimated by all participants by use of a linear regression analysis applied to hourly data

$$\frac{Q112+Q105}{H100} = F'\overline{\tau\alpha} - F'U_L\left(\frac{T100-T001}{H100}\right)$$

Results apply only to particular and limited conditions, depending on experiments and participants. They cannot be extrapolated to all conditions.

Some participants use more refined array efficiency expressions, to take into account the temperature dependence of the heat loss factor, heat pipe effects, or other effects. For instance

- $F'U_L = K_1+K_2\cdot\Delta T \Rightarrow \frac{Q112+Q105}{H100} = F'\overline{\tau\alpha} - (K_1+K_2\cdot\Delta T)\cdot\frac{\Delta T}{G001}$

$\Delta T = T100 - T001$

A bilinear fit, $\Delta T/G001$ and $\Delta T^2/G001$ being considered as independant variables, is used for the determination of $F'\overline{\tau\alpha}$, K_1 and K_2.

As seen previously for single ETC efficiencies, this parametrization induces a splitting of the efficiency curves η versus the usual variable $\Delta T/G001$.

- The previous temperature dependence may be parametrized by using a radiation model

$$\frac{Q112 + Q105}{H100} = F'\overline{\tau\alpha} - 2\overline{\varepsilon}\,\frac{A_{abs}}{A_{ap}}\,\sigma\,\frac{T100^4-T001^4}{G001}$$

with the same symbols as previously defined.

This parametrization applied to Swiss data (SOLARCAD) gives slightly larger optical efficiencies as compared to first case, compensated by larger heat losses (see Table 3-4).
It means that the whole set of parameters gives a coherent description of the experiment, but that an individual parameter may slightly depend on the modeling or the method used for its evaluation.

- Another participant, USA, Solar House I, using Philips VTR361 collectors, takes the following regression equation

$$\frac{Q112+Q105}{H100} = a + b\,\frac{\Delta T}{G001} + c\,\frac{\Delta T^2}{G001} + d\cdot\Delta T + e\cdot G001$$

This relation is similar to equation (3) given for single ETC efficiency.

- Also, the array thermal capacity may be evaluated by fitting procedures. For instance first case leads to

$$\frac{Q112}{H100} = F'\overline{\tau\alpha} - (K_1+K_2\cdot\Delta T)\,\frac{\Delta T}{G001} - C100\,\frac{\delta T}{G001}$$

where $\delta T = T100_n - T100_{n-1}$.

These procedures may be extended to other hourly data outside the period 11a.m. - 2p.m. Other effects may then appear; for instance, thermal capacity, incidence angle modifier, or shading. These effects may be investigated and evaluated by use of appropriate procedures. For instance, the array efficiency expression should include additional terms for the corresponding effects whith data fitted to such an expression. This situation is similar to the one already encountered when dealing with single ETC characteristics.

3.3 SHADING

Collector shading due to environment or mutual collector shading from collector raw to collector raw may occur in some experiments. It should be minimized by proper design.

Single ETC characteristics imply no shading effects. Absorber tilt angle effects are dealt with separately, as seen before.

Shading is typically an array problem. Shading effects should be dealt with and evaluated separately to facilitate relevant characterizations and comparisons.

Some ETC array characteristics may be extracted from those selected hourly data involving no shading effects. For the other array characteristics as well as for long-term array performances, it is necessary to consider and to evaluate the average effective solar radiation reaching the collectors. In other words shading losses must be evaluated properly. This procedure implies precautions and detailed computations such as:

- no shading on solarimeters
- separate beam/diffuse radiation treatment and modeling or assumptions for diffuse radiation
- geometrical considerations such as sun angles and motions, collector geometry and other considerations
- integration over time of all conditions.

Because conditions, geometries and problems are quite different from one experiment to the other, each participant applies his own corrections when necessary. Thus we do not present here a normalized and general method to deal with this problem. It is important to mention this problem and to apply the necessary corresponding corrections for a proper evaluation of characteristics and performances.

TABLE 3-1. COLLECTOR ARRAYS USED IN IEA-VI EXPERIMENTS.
GEOMETRICAL AND DESIGN FEATURES.

COUNTRY	INSTALLATION	ETC-TYPE	NB OF MODULES	←TOTAL AREA→ APERTURE [m²]	ABSORBER [m²]	COLL.PLANE TILT ANGLE [DEG]	ABS.PLANE TILT ANGLE [DEG]
AUSTRALIA	Sydney University	Sydney University	32	40.0	63.0	12.5	NA
CANADA	Mountain Springs	SOLARTEC	216	281.	248.	50	NA
C.E.C.	JRC ISPRA	Philips VTR361	3	6.81	3.8	30.	0.
		Philips VTR261	5	11.1	8.6	30.	0.
		Sanyo STC-CU250L	6	14.5	8.75	30.	0.
F.R.G.	Solarhaus Freiburg	Corning "US"	24	34.8	26.9	55.	0.
		Philips VTR261	15	29.2	16.4	55.	0.
NETHERLANDS	Eindhoven University	Philips VTR261	23	47.15	33.35	48.	0.
SWEDEN	Södertörn	Philips VTR141	88	120.6	NIA	60.	0.
		General Electric TC100	110	150.	NIA	40.	NA
		Teknoterm HT(F.P)	NIA	144.	NIA	40.	NA
		Gränges Aluminium(F.P)	90	191.	NIA	40.	NA
		Scandinavian Solar HT(F.P)	18	216.	NIA	43.	NA
	Knivsta	Philips VTR141	18	24.6	NIA	60.	0.
		General Electric TC100	28	38.4	NIA	45.	NA
		Owens Illinois Sunpak	14	35.6	NIA	45.	NA
		Scandinavian Solar HT(F.P)	2	24.0	NIA	45.	NA
SWITZERLAND	Solarcad District	Corning CORTEC"A"	6	8.7	6.72	30.	0.
		Corning CORTEC"B"	6	8.7	6.72	30.	0.
		Sanyo STC-CU250L	8	19.52	13.84	30.	0.
	Id. 1985 installation	Corning CORTEC"E"	708	1026.	793.	2.5	30.
SWITZERLAND	Solarin Industry	Corning CORTEC"D"	280	406.	313.6	2.	30.
U.S.A.	CSU Solar House I	Philips VTR361	24	54.5	30.4	45.	0.
		Philips VTR141	52	59.6	34.4	45.	0.

Notes : (1) Mutual collector shading (significant from November to February) taken into account.
(2) In the late afternoon in months of October, February and March: up to 20% of total area.
(3) Mutual shading of absorbers from tube to tube included in IAM-effects.
(4) West mountain cuts sun about 1/2 hour before sundown (No corrections).
No estimate of inter-row shading has been made.

LATITUDE OF SITE [DEG]	AZIMUT FACED BY ARRAY [DEG]	TUBE ORIENTATION	BACKGROUND BEHIND COLLECTORS	SHADOW EFFECTS
33.55°S	0°(North)	N-S	Flat, diffuse white	None
53.55°N	0°(South)	N-S	CPC Reflectors	No effect due to horizon[1]
	~0°(South)	N-S	Ripple refl. of Al.	No significant effect
	~0°(South)	N-S	Flat refl. of Al.	No significant effect
	~0°(South)	E-W	Grey painted steel	No significant effect
47.58°N	12.5West	E-W	Roof tiles(dark brown)	No shading
47.58°N	12.5West	N-S	Roof tiles(dark brown)	Less than 5% in late afternoon
51.48°N	7. West	N-S	Tedlar coated Alum.	Nearly House[2]
59.00°N	0°(South)	N-S	White gravel	Very small from adjacent rows
59.00°N	0°	N-S	CPC reflector	id.
59.00°N	0°	NA	NA	id.
59.00°N	0°	NA	NA	id.
59.00°N	0°	NA	NA	id.
59.44°N	0°	N-S	Black roof	Very small from adjacent rows
59.44°N	0°	N-S	CPC reflector	id.
59.44°N	0°	N-S	CPC reflector	id.
59.44°N	0°	NA	NA	id.
46.2 °N	4° West	E-W	White painted sheet	Mutual row shading : Nov. - Feb.
46.2 °N	4° West	E-W	Roof (grey)	Mutual row shading : Nov. - Feb.
46.2 °N	4° West	E-W	Roof (grey)	Mutual row shading : Now. - Feb.
46.2 °N	4° West	E-W	None(railroad 10m below)	Small effects due to nearly buildings +[3]
47.6 °N	0°(South)	E-W	Roof (white painted rocks)	None[3]
40.6 °N	0°(South)	N-S	Ripple Al reflector	West mountain[4]
40.6 °N	0°(South)	N-S	White painted wood	West mountain[4]

TABLE 3-2. COLLECTOR ARRAYS USED IN IEA-VI EXPERIMENTS.
FLUID FLOW AND PIPING CHARACTERISTICS.

COUNTRY	INSTALLATION	ETC-ARRAY	WORKING FLUID	GLOBAL FLUID[11] FLOW RATE [ℓ/h m²aperture]
AUSTRALIA	Sydney University	Sydney University	Water+corrosion inhibitor[1]	38
CANADA	Mountain Springs	SOLARTECH	Deionized Water[2]	30
C.E.C.	JRC ISPRA	Philips VTR361	Water	92
		Philips VTR261	Water	54
		Sanyo STC-CU250L	Water	43
F.R.G.	Solarhaus Freiburg	Corning "US"	Water+38% Propylenglycol	36-54
		Philips VTR261	Water+38% Propylenglycol	40-60
NETHERLANDS	Eindhoven University	Philips VTR261	Water[12]	4-23
SWEDEN	Södertörn	Philips VTR141	Water+10% Ethylenglycol	54
		General Electric TC100	Water+35% Ethylenglycol	26
		Teknoterm HT(F.P)	Water+35% Ethylenglycol	30
		Gränges Aluminium (F.P)	Water+35% Ethylenglycol	38
		Scandinavian Solar HT(F.P)	Water+50% Propylenglycol	4-17
	Knivsta	Philips VTR141	Water+30% Ethylenglycol	24
		General Electric TC100	Water+10% Ethylenglycol	42
		Owens Illinois SUNPAK	Water	37
		Scandinavian Solar HT(F.P)	Water+50% Propylenglycol	15
SWITZERLAND	Solarcad District	Corning CORTEC "A"	Water+25% Ethylenglycol	35
		Corning CORTEC "B"	Water+25% Ethylenglycol	35
		Sanyo STC-CU250L	Water+25% Ethylenglycol	30-45
	Id. 1985 Installation	Corning CORTEC "E"	Water+32% Ethylenglycol	22-30[8]
SWITZERLAND	Solarin Industry	Corning CORTEC "D"	Water+32% Propylenglycol[3]	25
U.S.A.	CSU Solar House I	Philips VTR361	Water+Ethylenglycol	40
		Philips VTR141	Water+50% antifreeze[4]	37

Notes : (1) Corrosion Inhibitor : MAXWELL CORAX. Complex Alkaline liquid formulation, concent. 670 ppm.
MAXWELL POLYMER 214 : mixture of an exclusive polymer and sequestering agent., concent. 670 ppm.
Freeze protection none necessary.
(2) Deionized water treated with "boron-nitrite" corrosion inhibitor.
(3) Propylene glycol is chosen for its lower toxicity (Swiss food industry control).
(4) Antifreeze for heating season only.
(5) 2 manifolds || in Tickelman, 12 collectors in series per manifold.
(6) 3 main rows of 236 collectors; in each row, parallel branches of 2 collectors in series.
(7) 7 main rows of 40 collectors; in each row, parallel branches of 2 collectors in series.
(8) One or two pumps running, depending on incident radiation (2 pumps above 500W/m²).

MODULE CONNECTION	TUBING MATERIAL	ELECTRICAL POWER OF ARRAY PUMP [W/m² aperture]	OPERATING MODE	OVERHEATING PROTECTION	REGULATION CRITERIUM (ON/OFF VALUES)
4 branches in // , per branch 2 series of 4 in //	Copper	9.5	Continuous flow	NIA	ΔT = 4.5/1.5°C
Every single tube in // with all others	Steel and copper	5.7	Drainback	Drainback	ΔT = 13.5/4.0°C (for > 40 min.)
Serie	galvanized steel	NIA	Continuous flow	NIA	NIA
Serie	galvanized steel	NIA	Continuous flow	NIA	NIA
3 groups of 2 coll in serie	galvanized steel	NIA	Continuous flow	NIA	NIA
2 groups of 12 coll. in serie(5)	Copper-Steel	10.2	Continuous flow	Exchanger on	G001(55°)>100W/m²
3 groups // of 5 coll. in serie	Copper-Steel	12.	Continuous flow	cold water mains	Time delayed OFF
Serie	Copper Ø22 O.D.	NIA	Continuous flow	Boiling out	NIA
Serie	Copper	16.6	Continuous flow	NIA	Coll. Pump ON
Parallel	Copper	6.7	Continuous flow	NIA	when T_{coll} > 40°C
Parallel	Copper	6.9	Continuous flow	NIA	
Parallel	Copper	5.2	Continuous flow	NIA	Heat delivery when
Parallel	Copper	4.6	Continuous flow	NIA	T_{coll} > T_{DH}
Series	Copper	2.0	Continuous flow	NIA	
Parallel	Copper	26.0	Continuous flow	NIA	Coll. Pump runs 24H
Parallel	Copper	28.1	Continuous flow	NIA	Heat delivery when
Parallel	Copper	42.0	Continuous flow	NIA	T_{coll} > T_{DH}
Parallel branches of	Steel	17.2	Continuous flow	Drain coll.(10)	
2 coll. in serie	Steel	17.2	Continuous flow	Drain coll.	G001>175W/m²
Parallel	Steel	15.4	Continuous flow	Drain coll.	
Parallel branches of(6)	Steel	3/1.5(8)	Continuous flow	Drain coll.(10)	G001>200/150W/m²(8)
2 coll. in serie					>500/450W/m²
Parallel branches of(7)	Steel	2.7	Continuous flow	Exchanger on	G011(30°Sud)>200/100W/m²
2 coll. in serie				cold water mains	
Serie	Copper	NIA	Continuous flow	NIA	NIA
4 branches of 13 in serie	Copper	4.2(9)	Continuous flow	Venting storage	NIA

(9) An early pump gave 1.6W/m², not sufficient to ensure balanced flow over the four branches.
(10) For pumping break safety only. District heating is always able to absorb all heat produced.
(11) Total flow divided by aperture area, whatever the module connections are.
(12) Freezing protection by recirculation.

TABLE 3-3. COLLECTOR ARRAYS USED IN IEA-VI EXPERIMENTS.
HEAT LOSSES AND THERMAL CAPACITANCE.

COUNTRY	INSTALLATION	ETC-ARRAY	FLUID VOLUME[1] IN PIPES [ℓ/m² aperture]	WORKING FLUID[1] CAPACITANCE IN PIPES C_{PF}[kJ/Km²ap]
AUSTRALIA	Sydney University	Sydney University	0.38	1.60
CANADA	Mountain Springs	SOLARTECH	0.78	3.2
C.E.C.	JRC ISPRA	Philips VTR361 Philips VTR261 Sanyo STC-CU250L	1.34	5.62
F.R.G.	Solarhaus Freiburg	Corning "US" Philips VTR261	1.26 1.29	4.88 5.01
NETHERLANDS	Eindhoven University	Philips VTR261	0.078	0.328
SWEDEN	Södertörn	Philips VTR141 General Electric TC100 Teknoterm HT(F.P) Gränges Aluminium (F.P) Scandinavian Solar HT(F.P)		
	Knivsta	Philips VTR141 General Electric TC100 Owens Illinois SUNPAK Scandinavian Solar HT(F.P)		
SWITZERLAND	Solarcad District	Corning CORTEC "A" Corning CORTEC "B" Sanyo STC-CU250L	0.66 0.86 0.99	2.77 3.61 4.16
	Id. 1985 Installation	Corning CORTEC "E"	1.14	4.45
SWITZERLAND	Solarin Industry	Corning CORTEC "D"	1.07	4.25
U.S.A.	CSU Solar House I	Philips VTR361 Philips VTR141	NIA NIA	NIA 0.03(7)

Notes : (1) Piping and other components from T101 to T102 (inlet and outlet temperature sensors for Q112 calculation), not including ETC's themselves.
(2) May differ from value of Table 2.3 if fluid used is not water.
(3) Including ETC's themselves. Night or other direct measurements, excluding hourly efficiency fit results.
(4) Insulation calculation, not including thermal bridges (no precise idea about them).
(5) Night heat loss measurement of piping and header pipes, excluding heat pipe tubes.
(6) Calculated from multilinear regression.
(7) Night measurements on heated solar loop.

PIPES EMPTY[1] CAPACITANCE C_{PE}[kJ/Km²ap]	TOTAL PIPING[1] CAPACITANCE $C_P=C_{PF}+C_{PE}$	TOTAL COLLECTOR[2] CAPACITANCE C_C[kJ/Km²ap]	TOTAL ARRAY CAPACITANCE $C_A=C_C+C_P$	PIPING HEAT[1] LOSS FACTOR CALCULATED U_P[W/Km²ap]	TOTAL ARRAY[3] CAPACITANCE MEASURED [kJ/Km²ap]	TOTAL ARRAY[3] HEAT LOSS MEASURED [W/Km²ap]
0.43	2.03	12.0	14.0	NIA	NIA	NIA
2.6	5.8	40.0	45.8	0.17	NIA	1.1±0.16
	Not significant Not significant					
0.92	6.54	10.0	16.5	NIA	NIA	0.33
1.06	5.94	3.94	9.9	NIA	11.6[6]	1.28
1.48	6.49	5.57	12.1	NIA	NIA	0.8 (5)
0.063	0.391	4.77	5.16	0.25	2.55	NIA
			NIA			
1.83	4.60	5.05	9.7	0.7	9.5	1.64 + 0.0096 ΔT[7]
2.40	6.01	5.05	11.1	0.7	10.6	1.98 + 0.017 ΔT[7]
2.78	6.94	7.5	14.4	0.8	10.6	1.85 + 0.012 ΔT[7]
0.92	5.37	5.05	10.4	0.06[4]	NIA	NIA
0.89	5.14	5.05	10.54	<0.1	9.6	1.33 + 0.008 ΔT[7]
NIA	NIA	NIA	NIA	NIA	NIA	NIA
0.011 (?)	NIA	0.48(?)	0.568(?)	NIA	NIA	NIA

TABLE 3-4. COLLECTOR ARRAYS USED IN IEA-VI EXPERIMENTS.
PARAMETER EVALUATION FROM HOURLY DATA

COUNTRY	INSTALLATION	ETC-ARRAY	MODEL USED TO FIT DATA
AUSTRALIA	Sydney University	Sydney University	$\frac{Q112+Q105}{H100} = F'\tau\alpha - F'U_L(\frac{\Delta T}{G00T})$ $(\Delta T=T100-T001)$
CANADA	Mountain Springs	SOLARTECH	$\frac{Q112+Q105}{H100} = F'\tau\alpha - F'U_L(\frac{\Delta T}{G00T})$
C.E.C.	JRC ISPRA	Philips VTR361 Philips VTR261 Sanyo STC-CU250L	
F.R.G.	Solarhaus Freiburg	Corning "US" Philips VTR261	$\frac{Q112+Q105}{H100} = F'\tau\alpha - F'U_L(\frac{\Delta T}{G00T})$
NETHERLANDS	Eindhoven University	Philips VTR261	$\frac{Q112+Q105}{H100} = F'\tau\alpha - F'U_L(\frac{\Delta T}{G00T}) - F'U_L U_{L_1}\Delta T$
SWEDEN	Södertörn	Philips VTR141 General Electric TC100 Teknoterm HT(F.P.) Gränges Aluminium (F.P.) Scandinavian Solar HT(F.P)	
	Knivsta	Philips VTR141 General Electric TC100 Owens Illinois SUNPAK Scandinavian Solar HT(F.P)	
SWITZERLAND	Solarcad District	Corning CORTEC"A"	(I) $\frac{Q112+Q105}{H100} = F'\tau\alpha - (K_1+K_2\Delta T)\ (\frac{\Delta T}{G00T})$
		Corning CORTEC"B"	(II) $\frac{Q112}{H100} = F'\tau\alpha \cdot IAM(b_0) - (K_1+K_2\Delta T)(\frac{\Delta T}{G00T}) - C100 \cdot \frac{\delta T}{H00T}$
		Sanyo STC-CU250L	(III) $\frac{Q112}{H100} = F'\tau\alpha \cdot IAM(b_0) - \varepsilon \cdot 2 \cdot \frac{A_{abs}}{A_{ap}} \cdot \sigma(\frac{T100^4 - T001^4}{G00T}) - C100 \cdot \frac{\delta T}{H00T}$
	id.1985 Installation	Corning CORTEC"E"	
SWITZERLAND	Solarin Industry	Corning CORTEC "D"	$\frac{Q112+Q105}{H100} = F'\tau\alpha - (K_1+K_2\Delta T)\ \frac{\Delta T}{G00T}$
U.S.A.	CSU Solar House I	Philips VTR361	$\frac{Q112}{H100} = F'\tau\alpha - (K_1+K_2\Delta T)\ \frac{\Delta T}{G00T} - d\Delta T - eG00I$
		Philips VTR141	$\frac{Q112+Q105}{H100} = F'\tau\alpha - F'U_L(\frac{\Delta T}{G00T})$

Notes : (1) C100 unit is kJ/K·m²ap (for H00I in kJ/m²ap and δT in K).
(2) $F'U_L$ probably underestimated and d overestimated by fit

	PARAMETERS		COMMENTS
$F'\tau\alpha$	$F'U_L$[W/ K·m²ap]	Others	
0.63	1.74		Values currently under investigation
0.42	1.01		Valid for $0.05 < \frac{\Delta T}{G00T} < 0.12$ km²/W, I > 850W/m², ΔT=50-100K
NIA			
NIA			
NIA			
0.66	1.39		Operation with both DHW and Heating temperature ranges.
0.65	1.19		Operation only within DHW-temperature range.
0.72	1.06	U_{L_1} = 1.33·10⁻³m²/W	U_{L_1} is the "heat loss resistance factor."
NIA			The system operation with near constant temperature does not give enough information for parameter evaluation methods.
NIA			
NIA			
NIA			
NIA			
NIA			
NIA			
NIA			
(I) 0.72	1.6+0.014ΔT	C100=9.5 (fixed)(1)	Expr. (I) is fitted on 11a.m.-2p.m. hourly data
(II) 0.71	1.7+0.011ΔT	C100=7.9	
(III)0.74	ε = 0.23	C100=9.2	(II) is fitted on 11a.m.- 5p.m. hourly data
(I) 0.60	2.2+0.012ΔT	C100=10.6(fixed)	
(II) 0.60	2.1+0.014ΔT	C100=7.1	(III) is fitted on 11a.m.- 5p.m. hourly data
(III)0.65	ε = 0.29	C100=8.8	
(I) 0.54	1.5+0.013ΔT	C100=10.6(fixed)	IAM(b_0) effect is simultaneously fitted in (II) and
(II) 0.53	1.5+0.011ΔT	C100=10.6	(III). See results on table I.5.
(III)0.58	ε = 0.23	C100=12.5	
NIA			
0.64	1.49+0.009ΔT		
0.680	0.6486+0.0035ΔT	d=7.055 10^{-3} $^{-1}$ (2)	100<G001<1200W/m², 30<ΔT<90K, stationary
0.50	1.46	e=11.3 10^{-6}m²/W	Winter data show smaller $F'U_L$ than summer ones.

4. COLLECTION SUBSYSTEM

From the array output to the collection subsystem output, diverse energy contributions, positive or negative, take place. They depend mainly on the following characteristics:

- heat loss factor, not including the array,
- thermal capacity, not including the array,
- pump characteristics such as power efficiency and other characteristics
- other characteristics which depend on the subsystem.

By knowing all significant characteristics about a single ETC, array, and collection subsystem, it is possible to predict the energy output from the collection subsystem for solar radiation, temperature, load and other given conditions. The whole procedure may be validated by measurements and then provides a useful design tool.

In Table 4-1, we present some information about collection subsystem characteristics for Task VI experiments.

TABLE 4-1. COLLECTOR SUBSYSTEMS IN IEA.VI EXPERIMENTS

Heat losses and thermal capacitances

COUNTRY	INSTALLATION	FLUID VOLUME [1] IN PIPES [liter/m²aperture]	FLUID CORRESPONDING[1] CAPACITANCE C_{TF} [kJ/Km²ap]	PIPES EMPTY[1] CAPACITANCE C_{TE} [kJ/Km²ap]	TOTAL PIPING[1] CAPACITANCE C_T [kJ/Km²ap]
AUSTRALIA	Sydney University	1.01	4.25	0.98	5.23
CANADA	Mountain Springs	0.91	3.7	1.8	5.5
C.E.C.	JRC ISPRA	0.9	3.66	0.84	4.50
F.R.G.	Solarhaus Freiburg	2.04[4]	7.7	7.1	14.8
NETHERLANDS	Eindhoven University				NIA
SWEDEN	Södertörn				NIA
	Knivsta				NIA
SWITZERLAND	Solarcad District[5]	2.2	9.2	3.3	12.5
	Solarcad District[6]	2.33	9.5	1.5	11.0
	Solarin Industry	0.97	3.84	2.33	6.17
U.S.A.	CSU Solar House I				NIA

Notes : (1) Includes piping, flowmeters, valves, pumps, heat exchangers of whole solar subsystem (between temperature sensors involved in Q102 evaluation), not including array's piping nor ETC's. If more than one array, the involved parameter is normalized to the sum of aperture areas.
(2) If more than one array, $C_a = \Sigma A_i C_{ai} / \Sigma A_i$ where A_i = aperture area of array i.
(3) Night measurements or others. Not including array nor ETC's.
(4) Because of the possible parallel operation of both arrays, installation is plumbed with 1 1/2 steel piping. With only one array, 1'' piping would have been used, leading to 0.91 ℓ/m² ap only.
(5) Early tests installation
(6) New 1000m² installation

TOTAL SUBSYSTEM[2] CAPACITANCE $C_S=C_T+CA$ [kJ/Km²ap]	PIPING HEAT[1] LOSS U_T [W/Km²ap]	SUBSYSTEM PIPING[3] CAPACITANCE MEASURED [kJ/Km²ap]	SUBSYSTEM PIPING[3] HEAT LOSS MEASURED [W/Km²ap]
NIA	NIA	NIA	NIA
51.3	0.18	NIA	<0.2
NIA	0.41	NIA	NIA
23.9	NIA	NIA	0.6
22.9	0.4	11.6	0.7
21.4	0.06	11.0	~ 0.07
16.71	0.055	5.0	0.081

5. SUMMARY AND PROGNOSIS

IEA Task VI has studied in detail the instantaneous, hourly, daily, monthly, and seasonal energy output from single collector arrays, and collection subsystems. The energy Input/Output diagrams, established on a daily basis, show a remarkably simple behaviour. These diagrams integrate all daily dynamic effects and can be considered as daily array characterizations. They can be used as a powerful and simple tool for designers, either directly or within a simple day-by-day simulation.

Also the same "Input-Output" diagrams may be constructed for the collection subsystem rather than for the array. Assume that by simple modeling you can deduce from system characteristics the daily collection subsystem characteristics, that is the energy output versus solar energy for given mean temperature difference between load an ambient, perhaps with additional small correction factors. Then, by use of a simple day-by-day simulation, including storage, load and other components, it is possible to predict the overall system performance. Further investigations along these lines are currently being carried out by the Task.

This daily analysis obviously depends on all characteristics mentioned in this report. Therefore, the following points are important:

- Identify all characteristics.
- Evaluate these characteristics in order to explain and understand measured performances.
- Optimize these characteristics when designing new projects.

This report has concentrated on developing standardized analytical performance evaluation procedures and characterizations for collector subsystems, arrays, and single collector modules. Because other subsystems may differ significantly from one participant to another, it has not gone very far into their characterization, but similar approaches could be productive. For more detail on subsystem and entire system performance and analyses, see other Task VI reports.